Exploring Natural Product Chemistry and Biology with Multicomponent Reactions. 5. Discovery of a Novel Tubulin-Targeting Scaffold Derived from the Rigidin Family of Marine Alkaloids

Liliya V. Frolova[*,†], **Igor V. Magedov**[†], **Anntherese E. Romero**[‡], **Menuka Karki**[§], **Isaiah Otero**[†], **Kathryn Hayden**[‡], **Nikolai M. Evdokimov**[†], **Laetitia Moreno Y. Banuls**[#], **Shiva K. Rastogi**[¶], **W. Ross Smith**[¶], **Shi-Long Lu**[Δ], **Robert Kiss**[#], **Charles B. Shuster**[§], **Ernest Hamel**[⊥], **Tania Betancourt**[¶], **Snezna Rogelj**[‡], and **Alexander Kornienko**[¶,*]

Departments of Chemistry and Biology, New Mexico Institute of Mining and Technology, Socorro, NM 87801, USA, Department of Biology, New Mexico State University, Las Cruces, NM 88003, USA, Laboratoire de Toxicologie and Laboratoire de Chimie Analytique, Toxicologie et Chimie Physique Appliquée, Institut de Pharmacie, Université Libre de Bruxelles, Brussels, Belgium, Departments of Otolaryngology, Dermatology and Pathology, University of Colorado, Anschutz Medical Campus, Aurora, CO 80045, USA, Screening Technologies Branch, Developmental Therapeutics Program, Division of Cancer Treatment and Diagnosis, National Cancer Institute, Frederick National Laboratory of Cancer Research, National Institutes of Health, Frederick, MD 21702, USA, Department of Chemistry and Biochemistry, Texas State University – San Marcos, San Marcos, TX 78666, USA

Abstract

We developed synthetic chemistry to access the marine alkaloid rigidins and over forty synthetic analogues based on the 7-deazaxanthine, 7-deazaadenine, 7-deazapurine and 7-deazahypoxanthine skeletons. Analogues based on the 7-deazahypoxanthine skeleton exhibited nanomolar potencies against cell lines representing cancers with dismal prognoses, tumor metastases and multidrug resistant cells. Studies aimed at elucidating the mode(s) of action of the 7-deazahypoxanthines in cancer cells revealed that they inhibited *in vitro* tubulin polymerization and disorganized microtubules in live HeLa cells. Experiments evaluating the effects of the 7-deazahypoxanthines on the binding of [^{3}H]colchicine to tubulin identified the colchicine site on tubulin as the most likely target for these compounds in cancer cells. Because many microtubule-targeting compounds are successfully used to fight cancer in the clinic, we believe the new chemical class of antitubulin agents represented by the 7-deazahypoxanthine rigidin analogues have significant potential as new anticancer agents.

---

[*]Corresponding authors. For L.V.F.: phone, +1 575 835 6886; fax, +1 575 835 5364; lfrolova@nmt.edu. For A.K.: phone, +1 512 245 3632; fax, +1 512 245 2374; a_k76@txstate.edu.
[†]Department of Chemistry, New Mexico Institute of Mining and Technology
[‡]Department of Biology, New Mexico Institute of Mining and Technology
[§]New Mexico State University
[#]Université Libre de Bruxelles
[Δ]University of Colorado
[⊥]National Cancer Institute
[¶]Texas State University

Introduction

In light of their fascinating novel structures, intriguing biological properties and the difficulty in obtaining large quantities from natural sources, marine pyrrole-derived alkaloids have attracted considerable attention from organic and medicinal chemists.[1–8] At present, several marine natural products are in clinical trials, and one drug, trabectedin, was recently approved in Europe as the first ever marine-derived anticancer agent.[9] In this context, the marine alkaloid rigidins A, B, C, D (Figure 1) and E isolated from the tunicate *Eudistoma cf. rigida* found near Okinawa and New Guinea have remained largely unexplored despite initial reports of promising biological activities.[10–12]

These compounds were shown to exhibit cytotoxicity against murine leukemia L1210 cells,[11] while rigidin A was also found to possess anticalmodulin activity.[10] Further work in this area was hampered by the miniscule isolation yields of these natural products (0.0015 % for A, 0.00031 % for B, 0.00008 % for C, 0.00004 % for D, and 0.018 % for E based on dry weight). Up to 2011, the synthetic accomplishments in the rigidin area included three total syntheses of rigidin A[13–16] and one of rigidin E.[16] These approaches involved lengthy synthetic sequences and/or low overall yields and did not offer a solution to the natural product supply problem. More importantly, however, the lack of synthetic flexibility impeded their use for the preparation of analogues for structure-activity relationship (SAR)[a] studies. Because our research program aims to develop multicomponent reactions (MCR) to access "privileged medicinal scaffolds,"[17–20] we became interested in the rigidins, which incorporate the purine-like pyrrolo[2,3-*d*]pyrimidine ring system, a common motif in natural products (e.g., tubercidin, toyocamycin, sangivamycin[21]) and medicinal agents with diverse bioactivities (e.g., anti-inflammatory,[22,23] anticancer,[24–29] antiviral,[30,31] adenosine A_1 and A_3 receptor inhibition,[32] adenosine kinase inhibition,[33,34] and dihydrofolate reductase inhibition[35]).

In 2011, we reported in a communication format a general total synthesis of rigidins A, B, C and D, which involved only four steps from commercially available materials and was amenable to the production of synthetic rigidin analogues.[36] This work has led to further developments and discoveries, which we describe here. More specifically, first, we detail the synthesis of first-generation synthetic analogues based on the 7-deazaxanthine skeleton. Second, we describe an anticancer evaluation of synthetically prepared rigidins A, B, C and D that, together with the first generation analogues, fail to display any significant effects on cancer cell proliferation. Third, we disclose novel MCRs leading to the preparation of the second-generation rigidin analogues based on the 7-deazaadenine, 7-deazapurine and 7-deazahypoxanthine (Figure 2) skeletons. Fourth, we show that the 7-deazahypoxanthines display potent antiproliferative activities. Fifth, we demonstrate that these compounds maintain their activity against tumor cells derived from cancers associated with dismal prognoses, metastatic tissues as well as multidrug resistant cells. Finally, we show that the anticancer properties of these hypoxanthine-like compounds are most likely caused by their pronounced effects on microtubule organization in cancer cells.

Results and Discussion

Chemistry

The synthesis of natural rigidins A, B, C and D, as well as synthetic 7-deazaxanthine analogues, is based on the chemistry shown in Table 1. Sulfonamides **6–11**, prepared by reacting commercially available aminoacetophenones with methanesulfonyl chloride, are utilized in a three-component reaction (3-CR) with various aromatic aldehydes **1–5** and cyanoacetamide in the presence of potassium carbonate in refluxing ethanol to give aminopyrroles **12–21** (Table 1). The synthesis of the 7-deazaxanthine framework is

completed by carbonylation with oxalyl chloride in diglyme to give analogues **22a–j** possessing diversely substituted aromatic moieties Ar^1 and Ar^2. Compounds **22a–d** are further hydrogenolyzed to yield natural rigidins with overall yields of 61% for A, 58% for B, 60% for C and 53% for D from commercially available aminoacetophenones. This sequence constitutes the first synthesis of rigidins B, C and D, while rigidin A is accessed via a significantly improved method compared with the previously described routes.[13–16] In addition, our reaction sequence leads to an expedient preparation of what we call the first-generation library of rigidin analogues based on the 7-deazaxanthine skeleton and possessing variable substituents in the aromatic moieties. Finally, in addition to these synthetic 7-deazaxanthines **22a–j**, we prepared a dithia variant **22k**, which is obtained by treating pyrrole **21** with carbon disulfide in pyridine (Figure 3).

Our further studies of the above-described three-component reaction led to the discovery of its four-component (4-CR) variants. Thus, we found that if the reaction is conducted in formamide as a solvent and cyanoacetamide is replaced with malononitrile (Table 2) or cyanomethylketones (Table 3), the entire pyrrolo[2,3-*d*]pyrimidine skeleton is assembled in one step giving rise to 7-deazaadenines **23** (Table 2) or 7-deazapurines **24** (Table 3), respectively. The success of these 4-CRs also depends on an optimized temperature regime, in which the reaction is first kept at 90 °C to allow for a clean formation of intermediate aminopyrroles (similar to **12–21** in Table 1) and then at 150 °C to bring the fourth component formamide into the process, leading to closure of the pyrimidine portion of the molecule.

Additionally, we discovered a 4-CR leading to the formation of a 7-deazahypoxanthine skeleton **25** (Table 4). In this modification, the starting sulfonamides, aldehydes and cyanoacetamide are reacted in a 1:1 mixture of EtOH and triethyl orthoformate under a similar temperature regime, involving reflux at 90 °C followed by a gradual increase in temperature to 150 °C, with the concomitant slow evaporation of ethanol.

The analogues accessed by these 4-CRs (Tables 2, 3 and 4) are generally obtained in good yields given the complexity of the newly devised reactions. The product pyrrolopyrimidines contain diversely substituted aromatic moieties, including alkoxy (e.g., **22a–i**, **23e**, **24a**, **25i–k**, **25q**, etc), halogen (e.g., **23a,b**, **25b–g**, **25r–t**, etc), cyano (e.g., **25o**) and heterocycles (e.g., **23b**, **25f–h**, **25v**, etc). Additionally, the hydroxy-substituted pyrrolopyrimidines can be obtained by the use of precursors containing benzyl-protected phenolic oxygens, with subsequent hydrogenolysis (similar to the synthesis of rigidins A–D from **22a–d** in Table 1) or through another modification in the MCR chemistry involving the use of HCOOH as the fourth component (Table 5). Formic acid plays a dual role, providing the necessary carbon for pyrimidine ring-closure and promoting *in situ* debenzylation of the phenolic benzyl ethers, resulting in analogues **25w–z** (Table 5). Interestingly, a search of the literature reveals no examples of metal-free utilization of formic acid for deprotection of benzyl ethers. To our knowledge the described chemistry represents the first examples of construction of the pyrrolo[2,3-*d*]pyrimidine skeleton in a one-step MCR process.

Pharmacology

(a) Antiproliferative Activities—The synthetically prepared natural products and their synthesized analogues were evaluated for antiproliferative activities using the HeLa cell line as a model for human cervical adenocarcinoma and MCF-7 cells as a model for breast adenocarcinoma. The cells were treated with each compound for 48 h, and cell viability was assessed using the MTT method[37] (Table 6). The natural alkaloids and synthetic 7-deazaxanthine **22e–k** analogues were inactive or weakly active, producing double-digit micromolar GI$_{50}$ values in some instances (e.g., analogue **22i**). Further, scaffold

modifications, such as those resulting in 7-deazaadenine analogues **23** and 7-deazapurine compounds **24**, led to the discovery of micromolar potencies associated with selected compounds (e.g., **23c** and **24c**). An unexpected and most gratifying observation was, however, the discovery of nanomolar antiproliferative activity in compounds based on the 7-deazahypoxanthine skeleton **25**. Thus, analogues **25a**, **25e**, **25g**, **25m** and **25u** all exhibited double-digit nanomolar potencies. A closer analysis of the SAR data indicates that the favored substitution pattern is the unsubstituted or para-substituted benzene ring at the sulfonamide-derived C-8 position (Ar^2) and either the unsubstituted or meta-halogen-substituted benzene group at the aldehyde-derived C-7 position (Ar^1). These structural features are found in the most potent analogues **25a–g**, **25m**, **25r–u**. The replacement of the Ph group at C-7 (as in **25a**) with the pyridine moiety (as in **25h**) led to a drop in potency by a factor of 15. Together, these data indicate that the C-7 and, possibly, C-8 aromatic groups bind in a pocket where hydrophobic interactions predominate, and introduction of hydrophilic pyridine nitrogen (**25h**) or hydroxyl groups (**25n, 25y,z**) leads to an unfavorable loss of solvation energy.

(b) Cell Cycle Analysis—The structural similarities between the rigidin analogues and previously described podophyllotoxin analogues,[19] as well as characteristic cellular morphological changes induced by the 7-deazahypoxanthines, led us to hypothesize that these compounds exert their antiproliferative properties through inhibition of tubulin dynamics, thus inducing mitotic arrest in cancer cells. To test this hypothesis, cell cycle analysis was performed using the cell permeable DNA binding dye Vybrant Orange. In a normal population, cells are distributed among the three major phases of the cell cycle, G_0/G_1, in which there is one set of paired chromosomes per cell (2n), followed by the S or synthesis phase, in which DNA is synthesized in preparation for division, and finally the G_2/M phase, in which the chromosomes of each cell have now been duplicated (4n). The DNA content can be measured by flow cytometry using fluorescent DNA selective probes such as Vybrant Orange that produce signals that are proportional to DNA mass per cell. Cell cycle analysis performed on HeLa cells using **25g** and **25m** with 0.1% dimethyl sulfoxide (DMSO) as a control revealed a pronounced cell cycle arrest in the G_2/M phase (Figure 4), and this effect is characteristic of antimitotic agents disrupting microtubule assembly.[38]

(c) Inhibition of tubulin assembly and colchicine binding to tubulin—To gain further insight into the possible antitubulin mechanism of action of the 7-deazahypoxanthines, the effects of these compounds on *in vitro* tubulin polymerization were assessed.[39] In our initial experiment, polymerization was followed by fluorescence enhancement due to the incorporation of a fluorescent reporter, in this case 4′,6-diamidino-2-phenylindole (DAPI), into microtubules as polymerization occurs. The test compounds were compared to three different controls, a known microtubule stabilizer (taxol), a known microtubule destabilizer (colchicine) as well as a solvent control sample. Whereas taxol induced potent enhancement of microtubule formation relative to the effect of the DMSO control, 7-deazahypoxanthines **25a** and **25m** displayed potent inhibition of microtubule assembly in a manner similar to the known tubulin polymerization inhibitor colchicine (Figure 5).

We next examined **25a** and **25m** in a quantitative turbidimetric assay,[40] in comparison with combretastatin A-4, a well-described potent inhibitor of the reaction (Table 7).[41] While **25a** differed little from combretastatin A-4 in its inhibitory effect, **25m** was distinctly less active. We also examined **25a** and **25m** for potential inhibitory effects on the binding of [³H]colchicine to tubulin (Table 7).[42] We found **25a** to be almost as active as combretastatin A-4, while **25m** was less active, in accord with their relative activities in the assembly assay.

There are three well-documented binding domains on tubulin, the first two of which include the pocket for taxanes and epothilones[43,44] and the pocket for vinca alkaloids.[45] FDA approved tubulin inhibitors binding to these two domains are all derivatives of complex natural products and are characterized by high bulkiness, hydrophobicity, and complicated structure. In addition, many tend to be easily recognized by P-glycoprotein (P-gp) and pumped out of cancer cells, which causes drug resistance.[46] The third binding domain of tubulin is the pocket for colchicine and podophyllotoxin, small natural products with relatively simple structures. So far, there are no FDA approved anticancer drugs targeting this domain,[47] although many colchicine site agents inhibit the growth of multidrug resistant (MDR) tumor cell lines and have reduced neurotoxicity and good oral bioavailability. These properties should be advantageous compared to the currently FDA approved tubulin inhibitors.[48–49] The results shown in Table 7 indicate that the 7-deazahypoxanthines, as represented by compounds **25a** and **25m**, constitute a new class of colchicine site agents.

(d) Microtubule organization in cells—To evaluate the effects of 7-deazahypoxanthines on the microtubule cytoskeleton in cells, we cultured HeLa cells in the presence of compounds **25a** and **25m** at a range of concentrations and examined microtubule morphology (Figure 6). At concentrations between 1 and 10 nM, interphase microtubule organization (Figure 6, panels A–C and M–O) was indistinguishable from DMSO controls (not shown). Similarly, mitotic spindle morphology and spindle length was unaffected at concentrations at or below 10 nM for both analogues. However, there was a pronounced change in both interphase and mitotic microtubule organization at concentrations between 10 and 100 nM, where both compounds caused a complete collapse of mitotic microtubule organization (Figure 6, Panel J–L and V–X). This was also the concentration range that encompassed the antiproliferative GI_{50} values for both compounds (GI_{50} (**25a**) = 35 nM, GI_{50} (**25m**) = 95 nM, Table 6). Additionally, while both compounds dramatically affected the polymerization and organization of dynamic mitotic microtubules, **25a** had a more drastic effect on interphase microtubule organization (Figure 6, panels D–F) in comparison with **25m** (Figure 6, Panels P–R), suggesting that **25a** was capable of affecting both dynamic and stable microtubule arrays. Together, these results lend further evidence indicating that tubulin-targeting is likely the main mechanism responsible for the antiproliferative effects of the 7-deazahypoxanthines.

(e) Aqueous Solubility—Because low aqueous solubility is an intrinsic property of many natural and synthetic drug candidates and is usually associated with poor absorption and bioavailability,[50,51] the water solubilities of the most potent nanomolar compounds **25a**, **25e**, **25g** and **25m** were determined with a UV/vis spectrophotometer at a wavelength of 335–336 nm. The solubility of compounds **25e**, **25g** and **25m** were 65 μM, 30 μM and 40 μM, respectively, while under the same conditions **25a** (10 μM) was less soluble. It appears that the *meta*-halogen substitution present in compounds **25e**, **25g** and **25m** is beneficial for the enhanced water solubility and will be considered for further development of this series of compounds. As a whole, these numbers fall in the range of water solubilities of the other reported colchicine-site targeting anti-tubulin compounds.[52]

(f) Activity against MDR cells—Because it is known that colchicine site agents are often insensitive to the action of P-gp,[53] we tested potent 7-deazahypoxanthines against MDR cells. The MDR uterine sarcoma cell line MES-SA/Dx5 was utilized for this experiment.[54] This cell line was established from the parent uterine sarcoma MES-SA, grown in the presence of increasing concentrations of doxorubicin and is known to be resistant to a number of P-gp substrates. Both taxol and vinblastine displayed more than a thousand fold drop in potency when tested for antiproliferative activity against the MDR cell line as compared with the parent line (Table 8). In contrast, there was only a small variation in the

sensitivities of the two cell lines towards 7-deazahypoxanthines **25a** and **25m**. Of note, the variation in sensitivity was slightly larger for the more lipophilic **25m** than that for **25a**, underscoring the idea that smaller, less lipophilic agents are poorer P-gp substrates.

(g) Activity against cancer cell lines representing cancers with dismal prognoses or derived from tumor metastases—To study the antiproliferative effects of our potent 7-deazahypoxanthines **25** further, we investigated whether they retained their potency against a panel of cancer cell lines, representing cancers known to be associated with dismal prognoses (Table 9). These include glioma (U373 and Hs683), melanoma (SKMEL-28 and B16F10), non-small-cell lung (NSCLC, A549) and head-and-neck cancers (UM-SCC10A and UM-SCC22A). In addition, because more than 90% of cancer deaths are caused by tumor metastases, two head-and-neck cancer cell lines derived from lymph node metastases (UM-SCC10B and UM-SCC22B) were added to the panel. 7-Deazahypoxanthines **25a**, **25g** and **25m** were found to retain their nanomolar potency against cells in this challenging *in vitro* panel (Table 9). Especially noteworthy are antiproliferative effects of **25a** against human glioma (U373) and melanoma (SKMEL-28) cells, which had single digit nanomolar GI_{50} values.

Conclusion

The research reported in this paper involves the utilization of the pyrrolo[2,3-*d*]pyrimidine-based natural alkaloid rigidins to discover novel anticancer agents. We described the development of novel synthetic chemistry allowing rapid access to various structural variants of this heterocyclic scaffold, which led to the generation of a library of diverse synthetic rigidin analogues. Although the natural products themselves were found to have little if any anticancer activity, synthetic analogues based on the 7-deazahypoxanthine skeleton were found to have promising double to single digit nanomolar antiproliferative potencies in human cancer cells. These compounds maintain potency in a panel of human cancer cells including those representing cancers with dismal prognoses as well as cells derived from metastatic lymph node tumors. All evidence obtained to date indicated that these rigidin analogues exert their antiproliferative action by inhibiting microtubule dynamics in cancer cells. Because many microtubule-targeting compounds are successfully used to fight cancer in the clinic, we believe the new chemical class of antitubulin agents represented by the 7-deazahypoxanthine rigidin analogues have significant potential as new anticancer agents.

Experimental Section

General Synthetic Methods

All reagents, solvents and catalysts were purchased from commercial sources (Acros Organics and Sigma-Aldrich) and used without purification. All reactions were performed in oven-dried flasks open to the atmosphere or under nitrogen and monitored by thin layer chromatography (TLC) on TLC precoated (250 μm) silica gel 60 F254 glass-backed plates (EMD Chemicals Inc.). Visualization was accomplished with UV light. Flash column chromatography was performed on silica gel (32–63 μm, 60 Å pore size). ^{1}H and ^{13}C NMR spectra were recorded on Jeol 300 or Bruker 400 spectrometers. Chemical shifts (δ) are reported in ppm relative to the TMS internal standard. Abbreviations are as follows: s (singlet), d (doublet), t (triplet), q (quartet), m (multiplet). HRMS analyses were performed at the Mass Spectrometry Facility, University of New Mexico or using Waters Synapt G2 LCMS. The synthesized compounds are at least 95% pure according to UPLC/MS analysis.

General Procedure for the Synthesis of 7-Deazaxanthines (22a–j)—A required pyrrole[36] (0.3478 mmol) was co-evaporated with 5 mL of toluene and dissolved in 3 mL of diglyme. Nitrogen gas was bubbled through the mixture for 5 min, and 0.20 mL (0.3825 mmol) of oxalyl chloride (2 M in CH_2Cl_2) was added dropwise while vigorously stirring the mixture. The mixture was refluxed for 10 h under nitrogen. After that time, the solvent was evaporated under reduced pressure, and 5 mL of 50% MeOH in CH_2Cl_2 was added to the solid in the flask. The precipitate was removed by filtration and rinsed sequentially with 2 mL of MeOH and 5 mL of diethyl ether. The mother liquor was chromatographed on silica gel using 30/1 to 30/5 CH_2Cl_2/MeOH gradient. The material from filtration and column chromatography was combined to give 7-deazaxanthines **22a–j**.

6-[4-(Benzyloxy)benzoyl]-5-[4-(benzyloxy)phenyl]-1*H*-pyrrolo[2,3-*d*]pyrimidine-2,4(3*H*,7*H*)-dione (22a): 81% as a brown powder, mp > 300 °C decomp. ^{1}H NMR (DMSO-d_6) δ: 5.02 (s, 2H), 5.06 (s, 2H), 6.69 (d, J = 8.8 Hz, 2H), 6.74 (d, J = 8.8 Hz, 2H), 7.07 (d, J = 8.7 Hz, 2H), 7.29–7.40 (m, 12H), 10.71 (bs, 1H), 11.31 (bs, 1H), 11.94 (bs, 1H). ^{13}C NMR (DMSO-d_6) δ: 69.8, 70.0, 98.9, 113.8, 114.3, 128.0, 128.1, 128.3, 128.5, 128.9, 129.0, 131.7, 132.8, 136.8, 137.6, 151.3, 158.1, 160.3, 161.2, 185.7. HRMS *m/z* (ESI$^+$) calc'd for $C_{33}H_{26}N_3O_5$ (M+H$^+$) 542.1721, found 542.1714.

6-[4-(Benzyloxy)-3-methoxybenzoyl]-5-[4-(benzyloxy)phenyl]-1*H*-pyrrolo[2,3-*d*]pyrimidine-2,4(3*H*,7*H*)-dione (22b): 74% as a brown powder, mp > 300 °C decomp. ^{1}H NMR (DMSO-d_6) δ: 3.57 (s, 3H), 5.01 (s, 2H), 5.05 (s, 2H), 6.72 (s, 1H), 6.87–7.10 (m, 7H), 7.37 (m, 10H), 10.72 (bs, 1H), 11.27 (bs, 1H), 11.94 (bs, 1H). ^{13}C NMR (DMSO-d_6) δ: 56.3, 70.3, 71.2, 99.1, 114.0, 114.1, 123.5, 125.4, 125.6, 127.9, 128.0, 128.2, 128.3, 128.9, 131.9, 132.8, 137.4, 137.8, 142.0, 149.2, 150.9, 151.7, 158.5, 160.1, 185.7. HRMS *m/z* (ESI$^+$) calc'd for $C_{34}H_{27}N_3NaO_6$ (M+Na$^+$) 596.1798, found 596.1792.

6-[4-(Benzyloxy)benzoyl]-5-[4-(benzyloxy)-3-methoxyphenyl]-1*H*-pyrrolo[2,3-*d*]pyrimidine-2,4(3*H*,7*H*)-dione (22c): 76% as a yellow powder, mp > 300 °C decomp. ^{1}H NMR (DMSO-d_6) δ: 3.60 (s, 3H), 4.97 (s, 2H), 5.03 (s, 2H), 6.66–6.74 (m, 5H), 7.34–7.38 (m, 12H), 10.70 (bs, 1H), 11.48 (bs, 1H), 11.96 (bs, 1H). ^{13}C NMR (DMSO-d_6) δ: 55.9, 70.0, 70.6, 98.9, 113.1, 114.2, 116.2, 124.4, 125.5, 125.8, 128.1, 128.3, 128.5, 128.9, 129.0, 129.1, 131.2, 131.6, 137.0, 137.7, 151.3, 160.3, 161.5, 185.8. HRMS *m/z* (ESI$^+$) calc'd for $C_{34}H_{27}N_3NaO_6$ (M+Na$^+$) 596.1798, found 596.1804.

6-[4-(Benzyloxy)-3-methoxybenzoyl]-5-[4-(benzyloxy)-3-(methoxy)phenyl]-1*H*-pyrrolo[2,3-*d*]pyrimidine-2,4(3*H*,7*H*)-dione (22d): 72% as a yellow powder, mp > 300 °C decomp. ^{1}H NMR (DMSO-d_6) δ: 3.52 (s, 3H), 3.55 (s, 3H), 4.98 (s, 2H), 5.04 (s, 2H), 6.74 (s, 1H), 6.78 (s, 1H), 6.88 (d, J = 8.4 Hz, 1H), 6.93 (d, J = 1.5 Hz, 1H), 7.10 (dd, J = 1.6 Hz, J = 8.3 Hz, 1H), 7.31–7.39 (m, 10H), 10.73 (bs, 1H), 11.27 (bs, 1H), 11.96 (bs, 1H). ^{13}C NMR (DMSO-d_6) δ: 55.6, 55.7, 70.5, 70.7, 98.8, 112.7, 113.2, 123.3, 124.3, 125.5, 125.6, 128.0, 128.1, 128.2, 128.4, 128.8, 128.9, 131.4, 137.0, 137.6, 141.9, 147.7, 148.1, 148.3, 151.1, 151.2, 160.2, 185.7. HRMS *m/z* (ESI$^+$) calc'd for $C_{35}H_{29}N_3NaO_7$ (M+Na$^+$) 626.1903, found 626.1908.

6-(4-Fluorobenzoyl)-5-(3,4,5-trimethoxyphenyl)-1*H*-pyrrolo[2,3-*d*]pyrimidine-2,4(3*H*, 7*H*)-dione (22e): 74%, mp > 300 °C decomp. ^{1}H NMR (DMSO-d_6) δ: 3.56 (s, 9H), 6.38 (s, 2H), 6.92 (m, 2H), 7.41 (m, 2H), 10.76 (bs, 1H), 11.32 (bs, 1H), 12.13 (bs, 1H). ^{13}C NMR (DMSO-d_6) δ: 55.5, 60.3, 99.2, 109.2, 113.8, 114.9, 126.1, 127.6, 130.0, 131.5, 137.2, 151.1, 160.5, 156.3, 185.5. HRMS *m/z* (ESI$^+$) calc'd for $C_{22}H_{18}FNaN_3O_6$ (M+Na$^+$) 462.1077, found 462.1064.

6-(4-Bromobenzoyl)-5-(3,4,5-trimethoxyphenyl)-1*H*-pyrrolo[2,3-*d*]pyrimidine-2,4(3*H*, 7*H*)-dione (22f): 64%, mp > 300 °C decomp. ^{1}H NMR (DMSO-d_6) δ: 3.50 (s, 9H), 6.33 (s, 2H), 7.23 (m, 4H). ^{13}C NMR (DMSO-d_6) δ: 56.2, 60.7, 99.4, 109.7, 125.1, 125.7, 127.5, 130.7, 130.8, 130.9, 137.7, 138.0, 142.4, 151.1, 151.9, 160.0, 185.6. HRMS *m/z* (ESI[+]) calc'd for $C_{22}H_{18}BrNaN_3O_6$ (M+Na^{+}) 524.0256, found 524.0259.

6-(4-Benzyloxy-3-methoxybenzoyl)-5-(3,4,5-trimethoxyphenyl)-1*H*-pyrrolo[2,3-*d*]pyrimidine-2,4(3*H*,7*H*)-dione (22g): 59%, mp > 300 °C decomp. ^{1}H NMR (DMSO-d_6) δ: 3.52 (s, 12H), 4.98 (s, 2H), 6.46 (m, 2H), 6.86 (m, 2H), 7.04 (m, 1H), 7.35 (m, 5H), 10.72 (bs, 1H), 11.25 (bs, 1H), 11.99 (bs, 1H). ^{13}C NMR (DMSO-d_6) δ: 55.5, 56.0, 70.4, 98.8, 109.6, 112.6, 112.7, 122.9, 125.8, 127.7, 128.0, 128.4, 128.9, 129.1, 131.2, 131.6, 137.0, 137.3, 148.1, 151.0, 151.7, 160.5, 185.8. HRMS *m/z* (ESI[+]) calc'd for $C_{30}H_{27}N_3NaO_8$ (M +Na^{+}) 580.1696, found 580.1697.

6-(4-Methoxybenzoyl)-5-(4-methoxyphenyl)-1*H*-pyrrolo[2,3-*d*]pyrimidine-2,4(3*H*,7*H*)-dione (22h): 76% as a yellow powder, mp > 300 °C decomp. ^{1}H NMR (DMSO-d_6) δ: 3.66 (s, 3H), 3.70 (s, 3H), 6.60 (d, *J* = 8.8 Hz, 2H), 6.67 (d, *J* = 8.8 Hz, 2H), 7.06 (d, *J* = 8.8 Hz, 2H), 7.37 (d, *J* = 8.8 Hz, 2H), 10.70 (bs, 1H), 11.32 (bs, 1H), 11.93 (bs, 1H). ^{13}C NMR (DMSO-d_6) δ: 55.7, 55.9, 70.0, 99.1, 113.1, 113.6, 125.0, 125.7, 128.9, 130.9, 131.6, 141.9, 151.1, 159.1, 160.2, 162.5, 185.8. HRMS *m/z* (ESI[+]) calc'd for $C_{21}H_{18}N_3O_5$ (M+H^{+}) 392.1246, found 392.1245.

6-Benzoyl-5-(4-methoxyphenyl)-1*H*-pyrrolo[2,3-*d*]pyrimidine-2,4(3*H*,7*H*)-dione (22i): 81% as a brown powder, mp > 300 °C decomp. ^{1}H NMR (DMSO-d_6) δ: 3.63 (s, 3H), 6.57 (d, *J* = 8.8 Hz, 2H), 7.01–7.13 (m, 5H), 10.73 (bs, 1H), 11.30 (bs, 1H), 11.99 (bs, 1H). ^{13}C NMR (DMSO-d_6) δ: 55.6, 99.4, 113.0, 124.7, 125.6, 128.1, 129.3, 130.1, 131.6, 132.8, 138.6, 142.3, 151.2, 159.1, 160.2, 186.9. HRMS *m/z* (ESI[+]) calc'd for $C_{20}H_{15}N_3NaO_4$ (M +Na^{+}) 362.1141, found 362.1141.

6-Benzoyl-5-(3,5-dibromophenyl)-1*H*-pyrrolo[2,3-*d*]pyrimidine-2,4(3*H*,7*H*)-dione (22j): 43%, mp > 300 °C decomp. ^{1}H NMR (DMSO-d_6) δ 7.14–7.35 (m, 8H), 10.8 (bs, 1H), 11.48 (bs, 1H), 12.37 (bs, 1H). ^{13}C NMR (DMSO-d_6) δ: 99.3, 121.2, 126.3, 126.7, 128.2, 129.0, 132.1, 133.2, 136.5, 138.4, 142.2, 151.2, 160.1, 186.6. HRMS *m/z* (ESI[+]) calc'd for $C_{19}H_{11}Br_2N_3NaO_3$ (M+Na^{+}) 511.9044, found 511.9052.

6-Benzoyl-5-(3,5-dibromophenyl)-1*H*-pyrrolo[2,3-*d*]pyrimidine-2,4(3*H*,7*H*)-dithione (22k): 57%, mp > 300 °C decomp. ^{1}H NMR (DMSO-d_6) δ: 7.30–7.47 (m, 10H), 8.63 (bs, 1H). ^{13}C NMR (DMSO-d_6) δ: 112.3, 120.8, 126.6, 128.1, 129.0, 132.1, 132.4, 133.9, 136.3, 138.1, 171.6, 187.1, 191.5. HRMS *m/z* (ESI[+]) calc'd for $C_{19}H_{12}Br_2N_3OS_2$ (M+H^{+}) 519.8789, found 519.8788.

Synthesis of Rigidins A, B, C and D—A selected benzyl-protected 7-deazaxanthine **22a–d** (0.0735 mmol) and Pd/C (20 mg, 10%) were suspended in DMF (0.3 mL) and MeOH (1 mL). The suspension was degassed three times by the freeze-pump-thaw method at −196 °C and then stirred under a hydrogen balloon for 3 h. After that time, the solvent was removed from the frozen sample by lyophilization, and the crude residue was dissolved in MeOH/CH$_2$Cl$_2$ and subjected to silica gel column chromatography (MeOH/CH$_2$Cl$_2$/ AcOH=10/50/1) to afford pure alkaloids.

6-(4-Hydroxybenzoyl)-5-(4-hydroxyphenyl)-1*H*-pyrrolo[2,3-*d*]pyrimidine-2,4(3*H*,7*H*)-dione (Rigidin A): 94.7% as a yellow solid, mp > 300 °C decomp. ^{1}H NMR (DMSO-d_6) δ: 6.46 (d, *J* = 8.5 Hz, 2H), 6.47 (d, *J* = 8.6 Hz, 2H), 6.94 (d, *J* = 8.5 Hz, 2H), 7.29 (d, *J* = 8.6

Hz, 2H), 9.28 (bs, 1H), 10.02 (bs, 1H), 10.63 (bs, 1H), 11.32 (bs, 1H), 11.84 (bs, 1H). ^{13}C NMR (CD$_3$OD) δ: 98.5, 113.6, 114.1, 123.9, 128.5, 129.3, 131.5, 132.3, 156.0, 160.2, 160.8, 162.9, 185.4. HRMS m/z (ESI$^+$) calc'd for C$_{19}$H$_{13}$N$_3$NaO$_5$ (M+Na$^+$) 386.0753, found 386.0742.

6-(4-Hydroxy-3-methoxybenzoyl)-5-(4-hydroxyphenyl)-1*H*-pyrrolo[2,3-*d*]pyrimidine-2,4(3*H*,7*H*)-dione (Rigidin B): 95% as a brown solid, mp > 300 °C decomp. ^{1}H NMR (DMSO-d_6) δ: 3.56 (s, 3H), 6.47 (d, J = 8.5 Hz, 2H), 6.57 (d, J = 8.2 Hz, 1H), 6.93 (d, J = 1.6 Hz, 1H), 6.99–7.01 (m, 3H), 9.30 (bs, 1H), 10.54 (bs, 1H), 11.99 (bs, 1H). ^{13}C NMR (DMSO-d_6) δ: 55.7, 98.8, 113.7, 114.3, 115.0, 123.6, 124.2, 125.3, 128.8, 129.6, 133.0, 147.0, 150.7, 152.7, 156.9, 160.7, 185.8. HRMS m/z (ESI$^+$) calc'd for C$_{20}$H$_{16}$N$_3$O$_6$ (M+H$^+$) 394.1039, found 394.1032.

6-(4-Hydroxybenzoyl)-5-(4-hydroxy-3-methoxyphenyl)-1*H*-pyrrolo[2,3-*d*]pyrimidine-2,4(3*H*,7*H*)-dione (Rigidin C): 96% as a dark yellow solid, mp > 300 °C decomp. ^{1}H NMR (DMSO-d_6) δ: 3.58 (s, 3H), 6.53 (m, 3H), 6.69–6.76 (m, 2H), 7.33 (d, J = 8.5 Hz, 2H), 8.69 (bs, 1H), 9.66 (bs, 1H), 10.21 (bs, 1H). ^{13}C NMR (DMSO-d_6) δ: 56.2, 98.7, 114.8, 115.6, 116.4, 123.5, 125.5, 129.3, 131.7, 132.1, 135.4, 141.8, 147.1, 148.1, 151.1, 161.1, 185.7. HRMS m/z (ESI$^+$) calc'd for C$_{20}$H$_{16}$N$_3$O$_6$ (M+H$^+$) 394.1039, found 394.1028.

6-(4-Hydroxy-3-methoxybenzoyl)-5-(4-hydroxy-3-methoxyphenyl)-1*H*-pyrrolo[2,3-*d*]pyrimidine-2,4(3*H*,7*H*)-dione (Rigidin D): 93% as a maroon solid, mp > 300 °C decomp. ^{1}H NMR (DMSO-d_6) δ: 3.52 (s, 3H), 3.54 (s, 3H), 6.49 (d, J = 8.1 Hz, 1H), 6.58 (d, J = 8.2 Hz, 1H), 6.66 (dd, J = 1.7 Hz, J = 8.1 Hz, 1H), 6.73 (d, J = 1.6 Hz, 1H), 6.93 (d, J = 1.6 Hz, 1H), 7.05 (dd, J = 1.6 Hz, J = 8.2 Hz, 1H), 8.89 (bs, 1H), 9.65 (bs, 1H), 10.60 (bs, 1H), 11.83 (bs, 1H). ^{13}C NMR (DMSO-d_6) δ: 55.8, 55.8, 98.8, 113.7, 114.7, 116.5, 123.7, 124.0, 124.8, 125.3, 128.8, 129.7, 146.3, 146.6, 146.9, 150.8, 160.6, 185.8. HRMS m/z (ESI$^+$) calc'd for C$_{14}$H$_7$N$_3$NaO$_7$ (M+Na$^+$) 446.0964, found 446.0964.

General procedure for the synthesis of 4-amino-7(*H*)pyrrolo[2,3-*d*]pyrimidines (7-deazaadenines 23a–f)— To a solution of *N*-(2-oxo-2-arylethyl)methanesulfonamide (2 mmol), the selected aldehyde (2.6 mmol) and malononitrile (2.6 mmol) in formamide (2 mL) was added anhydrous granulated K$_2$CO$_3$ (1.2 mmol) in one portion. The mixture was purged with nitrogen for 5 min and then heated at 100 °C for 24 hours under the nitrogen atmosphere. The formation of the intermediate pyrrole was monitored by TLC. After that, the reaction temperature was increased to 150 °C, and the reaction mixture was heated for 3–6 h. The mixture was cooled to room temperature and poured into water (30 mL). The formed precipitate was collected by filtration and washed with EtOH (2 mL) and diethyl ether (2 mL) to give the desired 7-deazaadenine **23a–f**.

4-Amino-6-benzoyl-5-(3,5-dibromophenyl)-7(*H*)pyrrolo[2,3-*d*]pyrimidine (23a): 58%, mp > 300 °C decomp. ^{1}H NMR (DMSO-d$_6$) δ: 7.23 (t, J = 7.41, 2H), 7.39 (m, 5H), 7.45 (d, J = 7.2 Hz, 2H), 8.24 (s, 1H),12.63 (s, 1H). ^{13}C NMR (DMSO-d$_6$) δ: 101.4, 119.7, 121.9, 127.5, 128.6, 129.2, 131.9, 132.2, 132.3, 137.1, 137.7, 150.9, 155.0, 158.8, 187.7. HRMS m/z (ESI$^+$) calcd for C$_{19}$H$_{13}$Br$_2$N$_4$O (M+H$^+$) 470.9456, found 470.9455.

4-Amino-6-benzoyl-5-(6-bromopyridin-2-yl)-7(*H*)pyrrolo[2,3-*d*]pyrimidine (23b): 66%, mp > 300 °C decomp. ^{1}H NMR (DMSO-d_6) δ: 6.37 (bs, 2H), 7.20 (m, 2H), 7.38 (m, 3H), 7.79 (s, 1H), 8.23 (s, 1H), 8.32 (s, 1H), 8.42 (s, 1H), 12.66 (s, 1H). ^{13}C NMR (DMSO-d_6) δ: 102.2, 118.0, 120.0, 128.3, 129.3, 130.1, 131.5, 132.4, 138.1, 140.5, 149.1, 149.2, 151.6,

155.5, 159.5, 188.1. HRMS *m/z* (ESI$^+$) calcd for $C_{18}H_{13}BrN_5O$ (M+H$^+$) 394.0303, found 394.0312.

4-Amino-6-benzoyl-5-phenyl-7(*H*)pyrrolo[2,3-*d*]pyrimidine (23c): 48%, mp 284 °C. ^{1}H NMR (DMSO-d$_6$) δ: 7.13 (m, 2H), 7.29 (m, 5H), 7.31 (m, 1H), 7.45 (d, *J* = 6.4 Hz, 2H), 7.97 (d, *J* = 8.8 Hz, 2H), 8.23 (s, 1H), 12.52 (s, 1H). ^{13}C NMR (DMSO-d$_6$) δ: 101.7, 122.5, 127.5, 127.6, 128.1, 128.9, 130.3, 131.7, 133.5, 137.5, 150.7, 154.9, 158.9, 162.9, 187.8. HRMS *m/z* (ESI$^+$) calcd for $C_{19}H_{15}N_4O$ (M+H$^+$) 315.1246, found 315.1238.

4-Amino-6-benzoyl-5-(thiophen-2-yl)-7(*H*)pyrrolo[2,3-*d*]pyrimidine (23d): 85%, mp 260 °C. ^{1}H NMR (DMSO-*d$_6$*) δ: 6.92 (m, 1H), 7.03 (s, 1H), 7.25 (t, *J* = 6.8 Hz, 2H), 7.4 (m, 3H), 7.58 (d, *J* = 7.4 Hz, 2H), 7.98 (d, *J* = 8.9 Hz, 1H), 8.24 (s, 1H), 12.65 (s, 1H). ^{13}C NMR (DMSO-d$_6$) δ: 102.0, 113.2, 127.5, 127.9, 128.2, 128.8, 129.5, 132.2, 133.6, 137.4, 150.6, 154.9, 158.8, 162.8, 187.7. HRMS *m/z* (ESI) calcd for $C_{17}H_{13}N_4OS$ (M+H$^+$) 321.0810, found 321.0801.

4-Amino-6-(3-cyanobenzoyl)-5-(4-benzyloxyphenyl)-7(*H*)pyrrolo[2,3-*d*]pyrimidine (23e): 54%, mp 252 °C. ^{1}H NMR (DMSO-*d$_6$*) δ: 5.12 (s, 2H), 6.82 (d, *J* = 8.08 Hz, 2H), 7.4 (m, 7H), 7.47 (d, *J* = 7.3 Hz, 2H), 7.67 (d, *J* = 6.5 Hz, 2H), 8.24 (s, 1H), 12.60 (s, 1H). ^{13}C NMR (DMSO-d$_6$) δ: 69.5, 69.5, 109.8, 114.1, 118.8, 119.6, 127.6, 128.0, 128.5, 129.4, 130.1, 131.3, 131.6, 131.9, 136.4, 138.7, 150.9, 154.5, 158.6, 161.6, 186.3. HRMS *m/z* (ESI$^+$) calcd for $C_{27}H_{20}N_5O_2$ (M+H$^+$) 446.1617, found 446.1609.

4-Amino-6-benzoyl-5-(2,6-dichlorophenyl)-7(*H*)pyrrolo[2,3-*d*]pyrimidine (23f): 72%, mp 262 °C. ^{1}H NMR (DMSO-*d$_6$*) δ: 7.22 (m, 3H), 7.35 (m, 3H), 7.49 (d, *J* = 6.7 Hz, 2H), 8.22 (s, 1H), 12.69 (s, 1H). ^{13}C NMR (DMSO-d$_6$) δ: 102.5, 116.5, 128.1, 128.4, 128.8, 129.5, 131.4, 131.9, 132.4, 135.7, 138.3, 151.9, 154.3, 155.8, 159.4, 187.7. HRMS *m/z* (ESI$^+$) calcd for $C_{19}H_{13}Cl_2N_4O$ (M+H$^+$) 383.0466, found 383.0474.

General procedure for the synthesis of 4-aryl-7(*H*)pyrrolo[2,3-*d*]pyrimidines (7-deazapurines 24a–e)—To a solution of the selected *N*-(2-oxo-2-arylethyl)methanesulfonamide (3 mmol), the selected arylcyanomethyl ketone (3.9 mmol), the selected aldehyde (3.9 mmol) in formamide (2 mL) was added anhydrous granulated K_2CO_3 (1.8 mmol). The mixture was purged with nitrogen and stirred overnight at 110 °C. The TLC monitoring of the reaction indicated the disappearance of the sulfonamide and the formation of the intermediate pyrrole (bright yellow spot on TLC). The temperature was then raised to 160 °C and the reaction was stirred for 3–6 h under nitrogen. After the pyrrole disappeared (TLC), the reaction mixture was cooled to room temperature and poured in a beaker with water (40 mL). The precipitate was collected by filtration and purified by column chromatography (CH_2Cl_2/EtOAc, 10:1) to yield the desired 7-deazapurine **24a–e**.

6-(4-Methoxybenzoyl)-4-(4-methoxyphenyl)-5-(4-Methoxyphenyl)-7(*H*)pyrrolo[2,3-*d*]pyrimidine (24a): 63%, mp 224 °C. ^{1}H NMR (DMSO-*d$_6$*) δ: 3.64 (s, 3H), 3.78 (s, 3H), 3.83 (s, 3H), 6.65 (s, 1H), 6.84 (d, *J* = 7.9 Hz, 2H), 6.96 (d, *J* = 8.0 Hz, 2H), 7.03 (d, *J* = 7.9 Hz, 2H), 7.38 (d, *J* = 8.0 Hz, 2H), 7.82 (d, *J* = 7.9 Hz, 2H), 8.13 (d, *J* = 7.9 Hz, 2H), 8.80 (s, 1H); ^{13}C NMR (DMSO-*d$_6$*) δ: 54.9, 55.1, 55.3, 113.7, 114.1, 115.4, 125.8, 126.9, 127.8, 129.1, 131.2, 133.3, 134.8, 146.8, 157.0, 158.6, 161.2, 173.7; HRMS *m/z* (ESI$^+$) calc'd for $C_{28}H_{24}N_3O_4$ (M+H$^+$) 466.1767, found 466.1761.

(5-(4-Methoxyphenyl)-4-phenyl-7*H*-pyrrolo[2,3-*d*]pyrimidin-6-yl)(phenyl)methanone (24b): 30%, mp 208 °C. ^{1}H NMR (DMSO-*d$_6$*) δ: 3.56 (s, 3H), 6.37 (d, *J* = 6.8 Hz, 1H), 6.66 (d, *J* = 6.8 Hz, 1H), 7.06 (dd, *J* = 8.2 Hz, 2H), 7.23 (m, 5H), 7.39 (t, *J* = 7.4 Hz, 1H), 7.53

(dd, *J* = 7.4 Hz, 2H), 8.99 (s, 1H); 13.03 (s, 1H). ^{13}C NMR (DMSO-*d*$_6$) δ: 55.4, 113.1, 114.5, 120.8, 125.4, 127.5, 128.4, 129.1, 129.7, 129.8, 132.1, 133.1, 137.1, 137.3, 152.14, 153.5, 158.5, 162.3, 189.8. HRMS *m/z* (ESI$^+$) calc'd for C$_{26}$H$_{19}$N$_3$O$_2$ (M+H$^+$) 406.1556, found 406.1557.

(5-(3,5-Dibromophenyl)-4-(*p*-tolyl)-7*H*-pyrrolo[2,3-*d*]pyrimidin-6-yl) (phenyl)methanone (24c): 33%, mp 250 °C. ^{1}H NMR (DMSO-*d*$_6$) δ: 2.27 (s, 3H), 6.90 (d, *J* = 1.7 Hz, 2H), 6.93 (d, *J* = 7.8 Hz, 1H), 7.10 (dd, *J* = 8.0 Hz, 2H), 7.25 (dd, *J* = 8.0 Hz, 2H), 7.37 (t, *J* = 1.7 Hz, 1H), 7.45 (t, *J* = 7.4 Hz, 1H), 7.55 (dd, *J* = 8.1 Hz, 2H), 9.01 (s, 1H); 13.25 (s, 1H). ^{13}C NMR (DMSO-*d*$_6$) δ: 20.9, 114.0, 118.0, 120.8, 127.8, 128.0, 128.9, 129.2, 131.1, 132.6, 132.9, 133.9, 136.6, 137.0, 138.9, 151.5, 151.5, 162.1, 188.8. HRMS *m/z* (ESI$^+$) calc'd for C$_{26}$H$_{18}$Br$_2$N$_3$O (M+H$^+$) 545.9817, found 545.9819.

(5-(3,5-Dibromophenyl)-4-phenyl-7*H*-pyrrolo[2,3-*d*]pyrimidin-6-yl)(phenyl)methanone (24d): 39%, mp 257 °C. ^{1}H NMR (DMSO-*d*$_6$) δ: 6.94 (d, *J* = 1.8 Hz, 2H), 7.13 (dd, *J* = 8.0 Hz, 2H), 7.25 (m, 5H), 7.35 (t, *J* = 1.7 Hz, 1H), 7.45 (t, *J* = 7.4 Hz, 1H), 7.55, (dd, *J* = 8.2 Hz, 2H), 9.03 (s, 1H); 13.29 (s, 1H). ^{13}C NMR (DMSO-*d*$_6$) δ: 114.4, 118.4, 121.3, 127.7, 128.4, 129.4, 129.6, 130.0, 131.7, 133.0, 133.3, 133.4, 137.1, 137.4, 152.0, 153.9, 162.4, 189.2. HRMS *m/z* (ESI$^+$) calc'd for C$_{25}$H$_{16}$Br$_2$N$_3$O (M+H$^+$) 531.9660, found 531.9653.

Phenyl(4-phenyl-5-(pyridin-3-yl)-7*H*-pyrrolo[2,3-*d*]pyrimidin-6-yl)methanone (24e): 22%, mp 232 °C. ^{1}H NMR (DMSO-*d*$_6$) δ: 6.82 (m, 1H), 7.03 (dd, *J* = 8.0 Hz, 2H), 7.20 (m, 6H), 7.42 (t, *J* = 7.4 Hz, 1H), 7.55 (dd, *J* = 8.2 Hz, 2H), 7.96, (d, = 1.08 Hz, 1H), 8.10, (dd, *J* = 4.8, Hz, 2H), 9.04 (s, 1H); 13.28 (s, 1H). ^{13}C NMR (DMSO-*d*$_6$) δ: 114.3, 117.2, 121.9, 127.3, 128.1, 129.0, 129.1, 129.2, 129.5, 132.9, 133.2, 132.9, 133.2, 136.6, 136.7, 137.5, 147.3, 150.5, 151.8, 153.4, 162.0, 188.9. HRMS *m/z* (ESI$^+$) calc'd for C$_{24}$H$_{17}$N$_4$O (M+H$^+$) 377.1402, found 377.1403.

General procedure for the synthesis of 1H-pyrrolo[2,3-d]pyrimidin-4(7H)-ones (7-deazahypoxanthines 25a–v)—To a solution of *N*-(2-oxo-2-arylethyl)methanesulfonamide (0.676 mmol), the selected aldehyde (0.879 mmol) and cyanoacetamide (0.072 g, 0.879 mmol) in a mixture of EtOH (2.5 mL) and HC(OEt)$_3$ (2.5 mL) was added anhydrous granulated K$_2$CO$_3$ (0.052g, 0.372 mmol) in one portion. The mixture was purged with nitrogen for 5 min and then heated at 90 °C for 24 hours under the nitrogen atmosphere. The formation of the intermediate pyrrole was monitored by TLC. After that the reaction temperature was increased to 150 °C, and the reaction mixture was heated for 3–6 h. The mixture was cooled to room temperature, and the formed precipitate was collected by filtration and washed with EtOH (2 mL) and diethyl ether (2 mL) to give the desired 7-deazahypoxanthine **25a–v**. An additional amount of the product was obtained by the evaporation of the mother liquor and purification of the residue by column chromatography with MeOH/CH$_2$Cl$_2$=1/40 to 1/20 gradient.

6-Benzoyl-5-phenyl-1*H*-pyrrolo[2,3-*d*]pyrimidin-4(7*H*)-one (25a): 71%, mp > 300 °C decomp. ^{1}H NMR (DMSO-*d*$_6$) δ: 7.04 (m, 3H), 7.15 (m, 4H), 7.33 (t, *J* = 6.8 Hz, 1H), 7.43 (d, *J* = 7.12 Hz, 2H), 8.02 (s, 1H), 12.01 (s, 1H), 12.79 (s, 1H). ^{13}C NMR (DMSO-d$_6$) δ: 106.3, 126.6, 126.7, 126.8, 127.5, 127.7, 129.0, 131.1, 131.8, 132.4, 137.4, 146.7, 149.3, 158.6, 187.7. HRMS *m/z* (ESI$^+$) calcd for C$_{19}$H$_{14}$N$_3$O$_2$ (M+H$^+$) 316.1086, found 316.1087.

6-Benzoyl-5-(3-iodophenyl)-1*H*-pyrrolo[2,3-*d*]pyrimidin-4(7*H*)-one (25b): 68%, mp > 300 °C decomp. ^{1}H NMR (DMSO-*d*$_6$) δ: 6.87 (t, *J* = 7.52 Hz, 1H), 7.19 (t, *J* = 7.44 Hz, 2H), 7.25 (d, *J* = 7.52 Hz, 1H), 7.42 (m, 5H), 8.04 (s, 1H), 12.90 (s, 1H), 12.09 (s, 1H). ^{13}C NMR (DMSO-*d*$_6$) δ: 93.0, 106.3, 125.0, 127.8, 128.7, 128.8, 130.4, 131.9, 134.6, 135.2, 137.4,

139.5, 146.9, 149.4, 158.5, 187.6. HRMS *m/z* (ESI$^+$) calcd for C$_{19}$H$_{13}$IN$_3$O$_2$ (M+H$^+$) 443.0086, found 443.0080.

6-Benzoyl-5-(3-chlorophenyl)-1*H*-pyrrolo[2,3-*d*]pyrimidin-4(7*H*)-one (25c): 61%, mp > 300 °C decomp. ^{1}H NMR (DMSO-*d$_6$*) δ: 7.04 (t, *J* = 7.48 Hz, 1H), 7.11 (d, *J* = 7.52 Hz, 2H), 7.19 (m, 3H), 7.38 (t, *J* = 6.2 Hz, 1H), 7.46 (d, *J* = 7.4 Hz, 2H), 8.04 (s, 1H), 12.05 (s, 1H), 13.00 (s, 1H). ^{13}C NMR (DMSO-*d$_6$*) δ: 106.4, 125.0, 126.5, 127.7, 128.5, 128.9, 129.7, 130.7, 131.5, 132.0, 134.6, 137.5, 146.8, 149.4, 158.5, 187.6. HRMS *m/z* (ESI$^+$) calcd for C$_{19}$H$_{13}$ClN$_3$O$_2$ (M+H$^+$) 350.0696, found 350.0694.

6-Benzoyl-5-(3-bromophenyl)-1*H*-pyrrolo[2,3-*d*]pyrimidin-4(7*H*)-one (25d): 54%, mp > 300 °C decomp. ^{1}H NMR (DMSO-*d$_6$*) δ: 7.00 (t, *J* = 7.08 Hz, 1H), 7.19 (m, 3H), 7.25 (d, *J* = 7.76 Hz, 1H), 7.34 (s, 1H), 7.38 (t, *J* = 6.96 Hz, 1H), 7.45 (d, *J* = 7.32 Hz, 2H), 8.04 (s, 1H), 12.05 (s, 1H), 12.90 (s, 1H). ^{13}C NMR (DMSO-*d$_6$*) δ: 106.4, 120.1, 124.9, 127.7, 127.8, 128.8, 128.9, 129.4, 132.0, 130.1, 133.6, 134.8, 137.4, 146.9, 149.3, 158.5, 187.5. HRMS *m/z* (ESI$^+$) calcd for C$_{19}$H$_{13}$BrN$_3$O$_2$ (M+H$^+$) 394.0191, found 394.0183.

6-Benzoyl-5-(3-fluorophenyl)-1H-pyrrolo[2,3-d]pyrimidin-4(7H)-one (25e): 53%, mp > 300 °C decomp. ^{1}H NMR (DMSO-*d$_6$*) δ: 7.08-6.88 (m, 2H), 7.19 (m, 1H), 7.36 (m, 1H), 7.46 (m, 2H), 7.61 (d, *J* = 7.2 Hz, 1H), 7.96 (d, *J* = 11.5 Hz, 1H), 8.01 (d, *J* = 7.2 Hz, 1H), 12.30 (s, 1H), 12.96 (s, 1H). ^{13}C NMR (DMSO-*d$_6$*) δ: 105.6, 114.1, 114.9, 115.1, 118.3, 124.5, 127.8, 129.0, 129.5, 131.2, 131.3, 132.5, 137.9, 159.8, 188.0. HRMS *m/z* (ESI$^+$) calcd for C$_{19}$H$_{13}$FN$_3$O$_2$ (M+H$^+$) 334.0992, found 395.0999.

6-Benzoyl-5-(6-bromopyridin-2-yl)-1*H*-pyrrolo[2,3-*d*]pyrimidin-4(7*H*)-one (25f): 60%, mp > 300 °C decomp. ^{1}H NMR (DMSO-*d$_6$*) δ: 7.19 (d, *J* = 8.0 Hz, 2H), 7.23 (d, *J* = 7.2 Hz, 2H), 7.40 (t, *J* = 6.4 Hz, 1H), 7.49 (d, *J* = 7.6 Hz, 2H), 7.61 (t, *J* = 7.6 Hz, 1H), 8.03 (s, 1H), 8.09 (d, *J* = 8.0 Hz, 1H), 12.17 (s, 1H), 13.05 (s, 1H). ^{13}C NMR (DMSO-*d$_6$*) δ: 105.5, 122.1, 124.6, 125.4, 128.0, 128.5, 129.7, 132.2, 137.8, 138.7, 139.3, 146.8, 149.3, 152.7, 158.8, 188.5. HRMS *m/z* (ESI$^+$) calcd for C$_{18}$H$_{12}$BrN$_4$O$_2$ (M+H$^+$) 395.0144, found 395.0125.

6-Benzoyl-5-(5-bromopyridin-3-yl)-1*H*-pyrrolo[2,3-*d*]pyrimidin-4(7*H*)-one (25g): 88%, mp > 300 °C decomp. ^{1}H NMR (DMSO-*d$_6$*) δ: 7.21 (d, *J* = 7.2 Hz, 2H), 7.38 (t, *J* = 6.4 Hz, 1H), 7.46 (d, *J* = 6.4 Hz, 2H), 7.81 (s, 1H), 8.05 (s, 1H), 8.31 (s, 1H), 8.35 (s, 1H), 12.12 (s, 1H), 13.01 (s, 1H). ^{13}C NMR (DMSO-d$_6$) δ: 107.3, 119.0, 121.9, 128.4, 129.1, 129.6, 131.1, 132.6, 138.0, 140.8, 147.6, 148.3, 150.0, 150.2, 159.2, 187.7. HRMS *m/z* (ESI$^+$) calcd for C$_{18}$H$_{11}$BrN$_4$NaO$_2$ (M+Na$^+$) 416.9963, found 416.9965.

6-Benzoyl-5-(pyridin-3-yl)-1*H*-pyrrolo[2,3-*d*]pyrimidin-4(7*H*)-one (25h): 61%, mp > 300 °C decomp. ^{1}H NMR (DMSO-*d$_6$*) δ: 7.08 (m, 1H), 7.18 (t, *J* = 7.24 Hz, 2H), 7.36 (t, *J* = 6.88 Hz, 1H), 7.46 (d, *J* = 7.12 Hz, 2H), 7.60 (d, *J* = 7.72 Hz, 1H), 8.06 (s, 1H), 8.23 (m, 1H), 8.31 (s, 1H), 12.12 (s, 1H), 13.00 (s, 1H). ^{13}C NMR (DMSO-*d$_6$*) δ: 106.7, 121.9, 123.0, 127.8, 127.9, 128.6, 129.2, 132.0, 137.3, 138.0, 147.0, 147.3, 149.5, 150.8, 158.6, 187.3. HRMS *m/z* (ESI$^+$) calcd for C$_{18}$H$_{13}$N$_4$O$_2$ (M+H$^+$) 317.1039, found 317.1038.

6-Benzoyl-5-(3,4,5-trimethoxyphenyl)-1*H*-pyrrolo[2,3-*d*]pyrimidin-4(7*H*)-one (25i): 64%, mp > 300 °C decomp., ^{1}H NMR (DMSO-*d$_6$*) δ: 3.32 (s, 3H), 3.54 (s, 3H), 3.56 (s, 3H), 6.46 (s, 2H), 7.16 (t, *J* = 8.0 Hz, 2H), 7.32 (t, *J* = 8.0 Hz, 1H), 7.44 (d, *J* = 7.7 Hz, 2H), 8.02 (m, 1H), 11.98 (s, 1H), 12.78 (s, 1H). ^{13}C NMR (DMSO-*d$_6$*) δ: 55.6, 59.7, 106.3, 109.4, 127.1, 127.5, 127.7, 128.8, 131.6, 137.8, 146.8, 149.4, 151.3, 158.5, 187.7. HRMS *m/z* (ESI$^+$) calcd for C$_{22}$H$_{20}$N$_3$O$_5$ (M+H$^+$) 406.1403, found 406.1390.

6-Benzoyl-5-(3-iodo-4,5-dimethoxyphenyl)-1*H*-pyrrolo[2,3-*d*]pyrimidin-4(7*H*)-one (25j): 37%, mp > 300 °C decomp. ^{1}H NMR (DMSO-d_6) δ: 3.58 (s, 6H), 6.82 (s, 1H), 7.07 (s, 1H), 7.16 (d, *J* = 7.6 Hz, 2H), 7.33 (t, 1H), 7.40 (d, *J* = 7.2 Hz, 2H), 8.02 (s, 1H), 12.00 (s, 1H), 12.85 (s, 1H). ^{13}C NMR (DMSO-d_6) δ: 56.1, 60.0, 91.3, 106.8, 117.2, 125.7, 128.1, 128.3, 129.2, 130.9, 132.2, 133.2, 138.2, 147.4, 147.6, 149.9, 150.9, 159.0, 188.1. HRMS m/z (ESI[+]) calcd for $C_{21}H_{17}IN_3O_4$ (M+H^{+}) 503.0297, found 503.0280.

6-Benzoyl-5-(3-bromo-4,5-dimethoxyphenyl)-1*H*-pyrrolo[2,3-*d*]pyrimidin-4(7*H*)-one (25k): 51%, mp > 300 °C decomp. ^{1}H NMR (DMSO-d_6) δ: 3.59 (s, 6H), 6.77 (s, 1H), 6.95 (s, 1H), 7.16 (d, *J* = 7.2 Hz, 2H), 7.34 (t, 1H), 7.41 (d, *J* = 7.2 Hz, 2H), 8.04 (s, 1H), 12.01 (s, 1H), 12.87 (s, 1H). ^{13}C NMR (DMSO-d_6) δ: 56.3, 60.2, 106.9, 115.5, 116.3, 125.8, 127.4, 128.0, 128.2, 129.2, 130.2, 132.2, 138.2, 145.0, 147.5, 150.0, 152.0, 159.0, 188.0. HRMS *m/z* (ESI[+]) calcd for $C_{21}H_{17}BrN_3O_4$ (M+H^{+}) 456.0382, found 456.0370.

6-Benzoyl-5-(2,6-dichlorophenyl)-1*H*-pyrrolo[2,3-*d*]pyrimidin-4(7*H*)-one (25l): 74%, mp > 300 °C decomp. ^{1}H NMR (DMSO-d₆) δ: 7.12 (d, *J* = 6.8 Hz, 2H), 7.20 (m, 3H), 7.34 (m, 1H), 7.47 (d, *J* = 6.0 Hz, 2H), 8.02 (s, 1H), 12.05 (s, 1H), 13.01 (s, 1H). ^{13}C NMR (DMSO-d₆) δ: 107.6, 120.2, 127.4, 127.5, 127.9, 128.2, 130.0, 132.0, 132.2, 135.3, 137.8, 147.6, 150.0, 158.0, 187.1. HRMS *m/z* (ESI) calcd for $C_{19}H_{12}Cl_2N_3O_2$ (M+H^{+}) 384.0307, found 384.0299.

6-Benzoyl-5-(3,5-dibromophenyl)-1*H*-pyrrolo[2,3-*d*]pyrimidin-4(7*H*)-one (25m): 77%, mp > 300 °C decomp. ^{1}H NMR (DMSO-d₆) δ: 7.23 (t, *J* = 7.24 Hz, 2H), 7.36 (s, 2H), 7.41 (t, *J* = 7.68 Hz, 1H), 7.46 (d, *J* = 7.68 Hz, 2H), 7.51 (s, 1H), 8.06 (s, 1H), 12.10 (s, 1H), 13.01 (s, 1H). ^{13}C NMR (DMSO-d₆) δ: 107.0, 107.1, 124.0, 128.3, 128.6, 129.3, 131.9, 132.6, 133.3, 137.0, 138.0, 147.6, 149.9, 159.0, 187.9. HRMS *m/z* (ESI[+]) calcd for $C_{19}H_{12}Br_2N_3O_2$ (M+H^{+}) 471.9296, found 471.9301.

6-Benzoyl-5-(3-hydroxyphenyl)-1*H*-pyrrolo[2,3-*d*]pyrimidin-4(7*H*)-one (25n): 26%, mp > 300 °C decomp. ^{1}H NMR (DMSO-d_6) δ: 6.43 (s, 1H), 6.51 (s, 1H), 6.65 (s, 1H), 6.76 (s, 1H), 7.17 (s, 2H), 7.34 (s, 1H), 7.45 (s, 2H), 7.98 (s, 1H), 9.08 (s, 1H), 11.97 (s, 1H), 12.72 (s, 1H). ^{13}C NMR (DMSO-d_6) δ: 106.7, 114.2, 118.6, 122.6, 127.0, 128.0, 128.2, 129.4, 132.4, 134.1, 138.0, 147.1, 149.7, 156.5, 159.0, 188.4. HRMS *m/z* (ESI[+]) calcd for $C_{19}H_{14}N_3O_3$ (M+H^{+}) 332.1035, found 332.1032.

3-(6-Benzoyl-4-oxo-4,7-dihydro-1*H*-pyrrolo[2,3-*d*]pyrimidin-5-yl)benzonitrile (25o): 47%, mp > 300 °C decomp. ^{1}H NMR (DMSO-d_6) δ: 7.19 (t, *J* = 7.64 Hz, 1H), 7.26 (t, *J* = 7.2 Hz, 1H), 7.38 (t, *J* = 6.64 Hz, 1H), 7.44 (d, *J* = 6.0 Hz, 2H), 7.51 (d, *J* = 6.96 Hz, 2H), 7.59 (s, 1H), 8.06 (s, 1H), 12.11 (s, 1H), 12.99 (s, 1H). ^{13}C NMR (DMSO-d_6) δ: 106.5, 109.9, 118.6, 118.6, 127.8, 128.0, 129.0, 130.2, 131.9, 133.8, 134.5, 135.8, 137.4, 147.0, 149.4, 158.6, 187.3. HRMS *m/z* (ESI[+]) calcd for $C_{20}H_{13}N_4O_2$ (M+H^{+}) 341.1039, found 341.1041.

5-(3,5-Dibromophenyl)-6-(4-fluorobenzoyl)-1*H*-pyrrolo[2,3-*d*]pyrimidin-4(7*H*)-one (25p): 56%, mp > 300 °C decomp. ^{1}H NMR (DMSO-d_6) δ: 7.03 (t, *J* = 8.0 Hz, 2H), 7.35 (s, 2H), 7.52 (t, *J* = 6.4 Hz, 2H), 7.56 (s, 1H), 8.05 (s, 1H), 12.11 (s, 1H), 13.02 (s, 1H). ^{13}C NMR (DMSO-d_6) δ: 80.3, 107.1, 115.5, 121.3, 124.4, 128.7, 132.0, 133.5, 134.9, 137.1, 147.9, 150.3, 159.4, 163.2, 166.1, 186.4. HRMS *m/z* (ESI[+]) calcd for $C_{19}H_{11}Br_2FN_3O_2$ (M+H^{+}) 489.9202, found 489.9182.

6-(4-Methoxybenzoyl)-5-(3,4,5-trimethoxyphenyl)-1*H*-pyrrolo[2,3-*d*]pyrimidin-4(7*H*)-one (25q): 56%, mp > 300 °C decomp. ^{1}H NMR (DMSO-d_6) δ: 3.32 (s, 3H), 3.56 (s, 6H),

3.71 (s, 3H), 6.51 (s, 2H), 6.71 (d, J = 9.6 Hz, 2H), 7.46 (d, J = 9.6 Hz, 2H), 8.01 (s, 1H), 11.97 (s, 1H). ^{13}C NMR (DMSO-d_6) δ: 56.0, 56.3, 60.4, 106.5, 110.0, 113.6, 126.4, 128.4, 131.9, 136.6, 146.9, 149.8, 152.1, 159.3, 162.8, 187.0. HRMS m/z (ESI[+]) calcd for $C_{23}H_{22}N_3O_6$ (M+H^{+}) 436.1509, found 436.1501.

5-(3,5-Dibromophenyl)-6-(4-methoxybenzoyl)-1H-pyrrolo[2,3-d]pyrimidin-4(7H)-one (25r): 60%, mp > 300 °C decomp., ^{1}H NMR (DMSO-d_6) δ: 3.77 (s, 3H), 6.79 (d, J = 8.36 Hz, 2H), 7.39 (s, 2H), 7.50 (d, J = 8.36 Hz, 2H), 7.57 (s, 1H), 8.04 (s, 1H), 12.01 (s, 1H), 12.92 (s, 1H). ^{13}C NMR (DMSO-d_6) δ: 55.5, 106.1, 113.3, 120.8, 122.3, 128.5, 129.9, 131.2, 131.4, 132.7, 136.6, 146.7, 149.1, 158.5, 162.5, 186.1. HRMS m/z (ESI[+]) calcd for $C_{20}H_{13}Br_2N_3NaO_3$ (M+Na^{+}) 523.9221, found 523.9221.

6-(4-(Benzyloxy)benzoyl)-5-(3,5-dibromophenyl)-1H-pyrrolo[2,3-d]pyrimidin-4(7H)-one (25s): 61%, mp 252 °C. ^{1}H NMR (DMSO-d_6) δ: 5.14 (s, 2H), 6.86 (d, J = 7.92 Hz, 2H), 7.36 (m, 3H), 7.41 (m, 4H), 7.56 (m, 3H), 8.04 (s, 1H), 12.15 (s, 1H), 12.95 (s, 1H). ^{13}C NMR (DMSO-d_6) δ: 69.4, 106.1, 106.2, 120.8, 122.3, 127.5, 127.9, 128.5, 130.0, 131.2, 131.4, 132.7, 136.5, 136.6, 146.7, 149.1, 158.5, 161.6, 186.0. HRMS m/z (ESI[+]) calcd for $C_{26}H_{17}Br_2N_3NaO_3$ (M+Na^{+}) 599.9534, found 599.9532.

6-(4-Bromobenzoyl)-5-(3,5-dibromophenyl)-1H-pyrrolo[2,3-d]pyrimidin-4(7H)-one (25t): 54%, mp 256 °C. ^{1}H NMR (DMSO-d_6) δ: 7.03 (d, J = 8.66 Hz, 2H), 7.36 (s, 2H), 7.52 (d, J = 8.06 Hz, 2H), 7.56 (s, 1H), 8.04 (s, 1H), 12.08 (s, 1H), 13.00 (s, 1H). ^{13}C NMR (DMSO-d_6) δ: 107.3, 114.9, 115.2, 121.2, 124.3, 131.4, 132.7, 132.9, 133.6, 135.4, 159.1, 163.2, 165.7, 186.1. HRMS m/z (ESI[+]) calcd for $C_{19}H_{11}Br_3N_3O_2$ (M+H^{+}) 549.8401, found 549.8395.

5-Benzoyl-6-(4-benzyloxyphenyl)-1H-pyrrolo[2,3-d]pyrimidin-4(7H)-one (25u): 68%, mp 246 °C. ^{1}H NMR (DMSO-d_6) δ: 5.07 (s, 1H), 6.77 (d, J = 8.3 Hz, 2H), 7.06 (m, 3H), 7.20 (m, 2H), 7.38 (m, 4H), 7.45 (d, J = 8.3 Hz, 2H), 7.98 (d, J = 3.7 Hz, 1H), 11.97 (s, 1H), 12.71 (s, 1H). ^{13}C NMR (DMSO-d_6) δ: 69.7, 106.6, 114.5, 125.8, 127.0, 127.4, 128.1, 128.2, 128.4, 128.9, 130.5, 131.5, 132.0, 133.1, 136.9, 1 46.8, 149.5, 159.1, 161.9, 186.9. HRMS m/z (ESI[+]) calcd for $C_{26}H_{20}N_3O_3$ (M+H^{+}) 422.1505, found 422.1502.

6-Benzoyl-5-(4-bromothiophen-2-yl)-1H-pyrrolo[2,3-d]pyrimidin-4(7H)-one (25v): 71%, mp 300 °C decomp., ^{1}H NMR (DMSO-d_6) δ: 6.95 (s, 1H), 7.33 (m, 2H), 7.48 (m, 2H), 7.58 (d, J = 6.9 Hz, 2H), 8.04 (s, 1H), 12.11 (s, 1H), 12.99 (s, 1H). ^{13}C NMR (DMSO-d_6) δ: 79.6, 79.6, 108.0, 117.0, 125.0, 128.5, 129.0, 129.3, 132.2, 133.0, 135.2, 137.9, 147.5, 149.8, 158.9, 187.9. HRMS m/z (ESI[+]) calcd for $C_{17}H_{10}BrN_3NaO_2S$ (M+Na^{+}) 421.9575, found 421.9568.

General procedure for the synthesis of 5-aryl-6-(4-hydroxybenzoyl)-1H-pyrrolo[2,3-d]pyrimidin-4(7H)-ones (7-deazahypoxanthines 25w–z)—To a solution of N-(2-oxo-2-arylethyl)methanesulfonamide (2 mmol), the selected aldehyde (2.6 mmol) and 2-cyanoacetamide (2.6 mmol) in ethanol (2 mL) was added anhydrous granulated K_2CO_3 (1.2 mmol) in one portion. The mixture was purged with nitrogen for 5 min and then refluxed for 24 hours under the nitrogen atmosphere. The formation of the intermediate pyrrole was monitored by TLC. After that, ethanol was evaporated under reduced pressure. To the dry residue, formic acid (4 mL) was added, and the mixture was refluxed for 24 hours. The formation of the 7-deazahypoxanthines **25w–z** was monitored by TLC. The mixture was cooled to room temperature and purified by flash chromatography to give the desired product.

6-(4-Hydroxybenzoyl)-5-phenyl-1*H*-pyrrolo[2,3-*d*]pyrimidin-4(7H)-one (25w): 88%, mp > 300 °C decomp., ^{1}H NMR (DMSO-d_6) δ: 6.52 (d, *J* = 7.88 Hz, 2H), 7.11 (m, 3H), 7.22 (m, 2H), 7.40 (d, *J* = 7.4 Hz, 2H), 7.99 (s, 1H), 10.17 (br.s, 1H), 11.93 (s, 1H), 12.66 (s, 1H). ^{13}C NMR (DMSO-d_6) δ: 106.0, 114.6, 124.6, 126.5, 126.9, 127.9, 128.3, 131.0, 131.9, 132.7, 146.2, 148.9, 158.8, 161.5, 186.7. HRMS m/z (ESI$^+$) calcd for $C_{19}H_{13}KN_3O_3$ (M+K$^+$) 370.0594, found 370.0595.

5-(3,5-Dibromophenyl)-6-(4-hydroxybenzoyl)-1*H*-pyrrolo[2,3-*d*]pyrimidin-4(7*H*)-one (25x): 70%, mp > 300 °C decomp. ^{1}H NMR (DMSO-d_6) δ: 7.42 (m, 4H), 7.57 (s, 1H), 7.61 (d, *J* = 7.8 Hz, 2H), 8.03 (s, 1H), 10.26 (s, 1H), 12.06 (s, 1H), 12.88 (s, 1H). ^{13}C NMR (DMSO-d_6) δ: 106.4, 115.2, 121.3, 122.0, 128.7, 129.1, 131.6, 132.3, 133.2, 137.2, 147.0, 149.4, 159.0, 162.2. HRMS *m/z* (ESI$^+$) calcd for $C_{19}H_{12}Br_2N_3O_3$ (M+H$^+$) 489.9225, found 489.9220.

6-(4-Hydroxybenzoyl)-5-(4-hydroxy-3-methoxyphenyl)-1*H*-pyrrolo[2,3-*d*]pyrimidin-4(7*H*)-one (25y): 64%, mp > 300 °C decomp., ^{1}H NMR (DMSO-d$_6$) δ: 3.54 (s, 3H), 6.76-6.47 (m, 5H), 7.39 (d, *J* = 8.1 Hz, 2H), 8.81 (s, 1H), 7.95 (s, 1H), 10.12 (s, 1H), 11.88 (s, 1H), 12.52 (s, 1H). ^{13}C NMR (DMSO-d$_6$) δ: 121.9, 115.7, 115.1, 114.4, 128.8, 134.4, 141.3, 146.6, 149.9, 154.4, 157.1, 159.8, 162.5, 168.1, 187.6. HRMS *m/z* (ESI$^+$) calcd for $C_{20}H_{15}KN_3O_5$ (M+K$^+$) 400.0909, found 400.0917.

6-(4-Hydroxybenzoyl)-5-(4-hydroxyphenyl)-1*H*-pyrrolo[2,3-*d*]pyrimidin-4(7*H*)-one (25z): 71%, mp > 300 °C decomp., ^{1}H NMR (DMSO-d_6) δ: 6.46 (d, *J* = 7.9 Hz, 2H), 6.51 (d, J = 7.9 Hz, 2H), 7.00 (d, *J* = 7.7 Hz, 2H), 7.37 (d, *J* = 7.7 Hz, 2H), 7.94 (s, 1H), 9.24 (s, 1H), 10.13 (s, 1H), 11.89 (s, 1H), 12.51 (s, 1H). ^{13}C NMR (DMSO-d$_6$) δ: 106.3, 114.3, 115.0, 123.8, 125.6, 127.8, 128.8, 129.0, 132.4, 132.7, 146.5, 149.3, 156.7, 159.2, 161.7, 186.0. HRMS *m/z* (ESI$^+$) calcd for $C_{19}H_{14}N_3O_4$ (M+H$^+$) 348.0984, found 348.0987.

Cell Culture

Human cancer cell lines were obtained from the American Type Culture Collection (ATCC, Manassas, VA, USA), the European Collection of Cell Culture (ECACC, Salisbury, UK) and the Deutsche Sammlung von Mikroorganismen und Zellkulturen (DSMZ, Braunschweig, Germany). The origin and histological type of each human cell line analyzed are as follows: glioma model lines were the Hs683 oligodendroglioma (ATCC code HTB-138) and the U373 glioblastoma (ECACC code 89081403) cell lines, melanoma model was the SKMEL-28 (ATCC code HTB-72) cell line, and carcinoma model was the A549 NSCLC (DSMZ code ACC107) cell line. Human cervical adenocarcinoma HeLa cells were cultured in DMEM supplemented with 10% fetal bovine serum (FBS). Human mammary carcinoma MCF-7 cells were cultured in DMEM supplemented with 10% FBS. Human uterine sarcoma MES-SA and MES-SA/Dx5 cells were cultured in RPMI-1640 medium supplemented with 10% FBS. The U373 cells were cultured in MEM culture medium (Lonza code 12-136F, Vervier, Belgium), while the Hs683, SKMEL-28 and A549 cells were cultured in RPMI culture medium (Lonza; code 12-115F) supplemented with 10% heat-inactivated FBS (Lonza, FBS South America code DE14-801F). Cell culture media were supplemented with 4 mM glutamine (Lonza code BE17-605E), 100 µg/mL gentamicin (Lonza code 17-5182), and penicillin-streptomycin (200 units/ml and 200 µg/ml) (Lonza code 17-602E). All cell lines were cultured in T25 flasks, maintained and grown at 37° C, 95% humidity, 5% CO_2.

Human head and neck cancer cell lines UMSCC10A, 10B, 22A and 22B were provided by Dr. Thomas Carey of University of Michigan under the MTA agreement with the University of Colorado. UMSCC10A and 22A were originated from the primary tumors of two

individual head and neck squamous cell carcinoma patients, and 10B and 22B were from their corresponding lymph node metastases. Cells were cultured in DMEM medium supplemented with 10% FBS, and antibiotics.

Antiproliferative Properties

To evaluate antiproliferative properties of the rigidins and rigidin analogues, the MTT assay was used. The HeLa, MCF-7, MES-SA, and MES-SA/Dx5 cell lines were assessed by trypsinizing each cell line and seeding 4×10^3 cells per well into microtiter plates. All compounds were dissolved in DMSO at a concentration of either 100 mM or 25 mM prior to cell treatment. The cells were grown for 24 h before treatment at concentrations ranging from 0.004 to 100 μM and incubated for 48 h in 200 μL media. 20 μL of MTT reagent in serum free medium (5 mg/mL) was added to each well and incubated further for 2 h. Media was removed, and the resulting formazan crystals were re-solubilized in 100 μL of DMSO. A_{490} was measured using a Thermomax Molecular Device plate reader. The experiments were performed in quadruplicate and repeated at least twice for each compound per cell line. Cells treated with 0.1% DMSO were used as a control, and phenyl arsine oxide (PAO) was used as a positive killing control.

For UMSCC-10A, 10B, 22A and 22B cells, the MTT assay was performed in a 24-well plate with 40000 cells in 500 uL media. The cells were grown for 24 h before treatment at concentrations ranging from 0.025 to 0.4 μM and incubated for additional 4 days. MTT was added for 3 h before harvest. A_{560} was measured using a BioTek plate reader. The experiments were performed in quadruplicate and repeated at least twice for each compound per cell line. Cells treated with 0.1% DMSO were used as a control.

Cell Cycle Analysis

To assess the effects of the analogues on the cell cycle, cell cycle analysis was performed by flow cytometry. 70–80 % confluent HeLa cells were trypsinized and seeded at an initial density of 2×10^5 cell per well into 6 well plates in DMEM supplemented with 10% FBS, 100 mg/L penicillin G and 100 mg/L streptomycin. The cells were allowed to adhere overnight before treatment with **25g** or **25m** at 1 μM. After 32 h, the cells were washed 3x with DMEM, trypsinized, pelleted, and re-suspended in 200 μL of culture medium containing 10 μM (2 μL/mL) Vybrant Orange dye. The samples in the labeling solution were transferred into Falcon tubes and incubated in a water bath for 30 min at 37 °C. The samples were then analyzed using a Becton Dickinson FACscan flow cytometer with CellQuest software. Cells treated with 0.1% DMSO were used as a control.

In Vitro Tubulin Polymerization Assay

To determine whether the compounds bind to tubulin, initial experiments were performed with the tubulin polymerization assay obtained from Cytoskeleton Inc. A 10x stock solution of each test compound (0.1% DMSO, taxol, colchicine, **25a** and **25m**) was prepared using molecular grade water. The tubulin reaction mix was prepared by mixing 243 μL of buffer 1 [80 mM PIPES sequisodium salt; 2.0 mM MgCl$_2$; 0.5 mM ethylene glycol-bis(2-aminoethyl ether)-N,N,N′,N′-tetraacetic acid, pH 6.9, 10 μM DAPI], 112 μL tubulin glycerol buffer (80 mM PIPES sequisodium salt; 2.0 mM MgCl$_2$; 0.5 mM ethylene glycol-bis(2-aminoethyl ether)-N,N,N′,N′-tetraacetic acid, 60% v/v glycerol, pH 6.9), 1 mM GTP (final concentration) and 2 mg/mL tubulin protein (final concentration). The reaction mixture was kept on ice until needed, but it was used within an hour of preparation. The 10x test compounds were pipetted into the corresponding wells and warmed in the plate reader for 1 min, after which time they were diluted with the reaction mixture to their final 1x concentrations and placed in the fluorescent plate reader. The test compounds were incubated with the tubulin reaction mixture at 37 °C each in a separate experiment. The

effect of each agent on tubulin polymerization was monitored in a temperature-controlled TECAN GENios Multifunction Fluorescence TRF, FI, FRET, Absorbance and Luminescence Microplate Reader for one hour, with readings acquired every 60 s.

Quantitative Effects on Tubulin Polymerization and on Colchicine Binding to Tubulin

To evaluate the quantitative effect of the compounds on tubulin assembly in vitro, varying concentrations of compounds were preincubated with 10 μM (1.0 mg/mL) bovine brain tubulin in 0.8 M monosodium glutamate (pH 6.6 in 2M stock solution) at 30 °C for 15 min and then cooled to 0 °C. After addition of 0.4 mM GTP, the mixtures were transferred to 0 °C cuvettes in recording spectrophotometers equipped with electronic temperature controller and rapidly (less than one minute) warmed to 30 °C. Tubulin assembly was followed turbidimetrically at 350 nm. The IC_{50} was defined as the compound concentration that inhibited the extent of assembly by 50% after a 20 min incubation. The methodology was described in detail previously.[40] The capacity of the test compounds to inhibit colchicine binding to tubulin was measured as described.[55] The reaction mixtures contained 1 μM tubulin, 5 μM [^{3}H]colchicine, and 5 or 1 μM test compound. Combretastatin A-4 was generously provided by Dr. G. A. Pettit, Arizona State University.

Morphological Analysis of Microtubule Organization in HeLa Cells

HeLa cells were cultured in EMEM (Lonza, Walkersville, MD) supplemented with 10% FBS (Atlanta Biologicals, Lawrenceville, GA), sodium pyruvate and sodium bicarbonate. For compound treatments, cells were treated for 3 h with either carrier (0.1% DMSO) or compounds solubilized in DMSO and prediluted in media prior to fixation by immersion in methanol at −20°C for 30 min. Cells were subsequently rehydrated in phosphate-buffered saline (1XPBS), and blocked by incubation in 3% bovine serum albumin (dissolved in 1XPBS) for one hour at room temperature. Cells were then incubated overnight at 4 °C with mouse anti-tubulin antibody (Sigma) and rabbit anti-pericentrin antibody (Abcam, Cambridge, MA) in blocking buffer. Primary antibodies were detected using Alexafluor-conjugated secondary antibodies (Molecular Probes), while DNA was detected using Hoechst 33342 (Invitrogen). All images were acquired using a Zeiss Axiovert 200M inverted microscope equipped with epifluorescence optics and an Apotome module (Carl Zeiss). Acquired images were then exported into eight bit tiff files, and figures were prepared using Adobe Photoshop software.

Water Solubility

A known mass of each molecule was dispersed in ultrapure deionized water (Millipore) at a concentration > 0.5 mg/mL. The supersaturated mixtures were sonicated for 1 minute in a bath sonicator and allowed to equilibrate for > 24 hours at room temperature. The supersaturated mixtures were then centrifuged for 10 minutes at 10,000 rpm (9,391 × g) in an Eppendorf microcentrifuge to remove the insoluble fraction of the drug. The supernatant was centrifuged further in a separate tube and the centrifugation process was repeated until no pellet was visible. The solution of the drug was then diluted in dimethyl sulfoxide (DMSO) at a 1:2 volume ratio of solution-to-DMSO. The concentration of the molecule in the water/DMSO solution was determined based on a concentration-absorbance calibration line created with solutions of the drug in a 1:2 water/DMSO co-solvent system. The peak absorbance of the drug (335–336 nm) was used to create the calibration. The water solubility of the drug was then determined by taking into account the dilution performed with the addition of DMSO.

Selection of Doxorubicin Resistant Cells

To assess the effects of the hypoxanthine-like rigidin analogues on MDR cells, the MES-SA/Dx5 cell line had to first be selected for. This was done according to Harker et al.[52] The cells were split and allowed to adhere overnight. The next day cells were initially exposed to a DOX concentration of 100 nM, which represented the GI_{50} concentration. The cells were maintained at this DOX concentration until their growth rate reached that of the untreated cells. The DOX concentration was then increased in two-fold increments and following the same growth criteria at each concentration. A final DOX concentration of 500 nM was used as the stopping point. Each new DOX concentration required approximately 2 passages to reach the growth rate of the untreated cells.

Supplementary Material

Refer to Web version on PubMed Central for supplementary material.

Acknowledgments

Abbreviations Used

ATCC	American Type Culture Collection
3-CR	three-component reaction
4-CR	four-component reaction
DAPI	4′,6-diamidino-2-phenylindole
DMEM	Dulbecco's modified Eagle's medium
DMF	dimethylformamide
DMSO	dimethyl sulfoxide
DSMZ	Deutsche Sammlung von Mikroorganismen und Zellkulturen
ECACC	European Collection of Cell Culture
EDTA	diaminoethanetetraacetic acid
EtOH	ethanol
FBS	fetal bovine serum
FITC	fluorescein isothiocyanate
FOG	Ficol Orange G
HEPES	4-(2-hydroxyethyl)-1-piperazinethanesulfonic acid
HHB	Heinz-HEPES buffer
HRMS	high resolution mass spectrometry
MCR	multicomponent reaction
MDR	multidrug resistant

MTT	3-(4,5-dimethylthiazol-2-yl)-2,5-diphenyltetrazolium bromide
PAO	phenyl arsine oxide
P-gp	P-glycoprotein
SAR	structure-activity relationship
TLC	thin layer chromatography
SD	standard deviation

References

1. Urban S, Hickford SJH, Blunt JW, Munro MHG. Bioactive marine alkaloids. Curr Org Chem. 2000; 4:765–807.

2. Hill RA. Marine natural products. Annu Rep Prog Chem Sect B. 2005; 1001:124–136.

3. Simmons TL, Andrianasolo E, McPhail K, Flatt P, Gerwick WH. Marine natural products as anticancer drugs. Mol Cancer Ther. 2005; 4:333–342. [PubMed: 15713904]

4. Dembitsky VM, Gloriozova TA, Poroikov VV. Novel antitumor agents: marine sponge alkaloids, their synthetic analogs and derivatives. Mini-Rev Med Chem. 2005; 5:319–336. [PubMed: 15777266]

5. Nakao Y, Fusetani N. Enzyme inhibitors from marine invertebrates. J Nat Prod. 2007; 70:679–710.

6. Sugumaran M, Robinson WE. Bioactive dehydrotyrosyl and dehydrodopyl compounds of marine origin. Mar Drugs. 2010; 8:2906–2935. [PubMed: 21339956]

7. Fan H, Peng J, Hamann MT, Hu J-F. Lamellarins and related pyrrole-derived alkaloids from marine organisms. Chem Rev. 2008; 108:264–287.

8. Ploypradith M, Batsomboon P, Ruchirawat S, Ploypradith P. Cytotoxicities and structure-activity relationships of natural and unnatural lamellarins toward cancer cell lines. Chem Med Chem. 2009; 4:457–465.

9. Mabuchi S, Hisamatsu T, Kawase C, Hayashi M, Sawada K, Mimura K, Takahashi K, Takahashi T, Kurachi H, Kimura T. The activity of trabectedin as a single agent or in combination with everolimus for clear cell carcinoma of the ovary. Clin Cancer Res. 2011; 17:4462–4473.

10. Kabayashi J, Cheng J, Kikuchi Y, Ishibashi M, Yamamura S, Ohizumi Y, Ohta T, Nozoe S. Rigidin, a novel alkaloid with calmodulin antagonistic activity from the Okinawan marine tunicate Eudistma CF. Rigida Tetrahedron Lett. 1990; 31:4617–4620.

11. Tsuda M, Nozawa K, Shimbo K, Kobayashi J. Rigidins B-D, new pyrrolopyrimidine alkaloids from a tunicate Cystodytes species. J Nat Prod. 2003; 66:292–294.

12. Davis RA, Christensen LV, Richardson AD, Moreira da Rocha R, Ireland CM. Rigidin E, a new pyrrolopyrimidine alkaloid from a Papua New Guinea tunicate Eudistoma species. Mar Drugs. 2003; 1:27–33.

13. Edstrom ED, Wei Y. Synthesis of a novel pyrrolo[2,3-*d*]pyrimidine alkaloid, rigidin. J Org Chem. 1993; 58:403–407.

14. Sakamoto T, Kondo Y, Sato S, Yamanaka H. Total synthesis of a marine alkaloid, rigidin. Tetrahedron Lett. 1994; 35:2919–2920.

15. Sakamoto T, Kondo Y, Sato S, Yamanaka H. Condensed heteroaromatic ring systems. Part 24. Synthesis of rigidin, a pyrrolo[2,3-*d*]pyrimidine marine alkaloid. J Chem Soc, Perkin Trans I. 1996:459–464.

16. Gupton JT, Banner EJ, Scharf AB, Norwood BK, Kanters RPF, Dominey RN, Hempel JE, Kharlamova A, Bluhn-Chertudi I, Hickenboth CR, Little BA, Sartin MD, Coppock MB, Krumpe KE, Burnham BS, Holt H, Du KX, Keertikar KM, Diebes A, Ghassemi S, Sikorski JA. The application of vinylogous iminium salt derivatives to an efficient synthesis of the pyrrole containing alkaloids rigidin and rigidin E. Tetrahedron. 2006; 62:8243–8255.

17. Magedov IV, Kireev AS, Jenkins AR, Evdokimov NM, Lima DT, Tongwa P, Altig J, Steelant WFA, Van slambrouck S, Antipin MY, Kornienko A. Structural simplification of bioactive natural

products with multicomponent synthesis. 4. 4*H*-Pyrano-[2,3-*b*]naphthoquinones with anticancer activity. Bioorg Med Chem Lett. 2012; 22:5195–5198. [PubMed: 22819765]

18. Magedov IV, Kornienko A. Multicomponent reactions in alkaloid-based drug discovery. Chem Heterocycl Comp. 2012:38–43.

19. Magedov IV, Frolova L, Manpadi M, Bhoga UD, Tang H, Evdokimov NM, George O, Georgiou KH, Renner S, Getlic M, Kinnibrugh TL, Fernandes MA, Van slambrouck S, Steelant WFA, Shuster CB, Rogelj S, van Otterlo WAL, Kornienko A. Anticancer properties of an important drug lead podophyllotoxin can be efficiently mimicked by diverse heterocyclic scaffolds accessible via one-step synthesis. J Med Chem. 2011; 54:4234–4246. [PubMed: 21615090]

20. Evdokimov NM, Van slambrouck S, Heffeter P, Tu L, Le Calve B, Lamoral-Theys D, Hooten CJ, Uglinskii PY, Rogelj S, Kiss R, Steelant WFA, Berger W, Yang JJ, Bologa CJ, Kornienko A, Magedov IV. Structural simplification of bioactive natural products with multicomponent synthesis. 3. Fused uracil-containing heterocycles as novel topoisomerase-targeting agents. J Med Chem. 2011; 54:2012–2021. [PubMed: 21388138]

21. Gupta PK, Daunert S, Nassiri MR, Wotring LL, Drach JC, Townsend LB. Synthesis, cytotoxicity, and antiviral activity of some acyclic analogues of the pyrrolo[2,3-*d*]pyrimidine nucleoside antibiotics tubercidin, toyocamycin, and sangivamycin. J Med Chem. 1989; 32:402–408. [PubMed: 2913300]

22. Mohamed MS, Kamel R, Fatahala SS. Synthesis and biological evaluation of some thio-containing pyrrolo[2,3-*d*]pyrimidine derivatives for their anti-inflammatory and anti-microbial activities. Eur J Med Chem. 2010; 45:2994–3004.

23. Mohamed MS, Rashad AE, Adbel-Monem M. New anti-inflammatory agents. Z Naturforsch. 2007; 62c:27–31.

24. Abou El Ella DA, Ghorab MM, Noaman E, Heiba HI, Khalil AI. Molecular modeling study and synthesis of novel pyrrolo[2, 3-*d*]pyrimidines and pyrrolotriazolopyrimidines of expected antitumor and radioprotective activities. Bioorg Med Chem. 2008; 16:2391–2402. [PubMed: 18086527]

25. Willemann C, Grunert R, Bednarski PJ. Synthesis and cytotoxic activity of 5,6-heteroaromatically annulated pyridine-2,4-diamines. Bioorg Med Chem. 2009; 17:4406–4419. [PubMed: 19481463]

26. Tangeda SJ, Garrlapati A. Synthesis of new pyrrolo[2,3-*d*]pyrimidine derivatives and evaluation of their activities against human colon cancer cell lines. Eur J Med Chem. 2010; 45:1453–1458. [PubMed: 20163895]

27. Ghorab MM, Ragab FA, Heiba HI, Youssef HA, El-Gazzar MG. Synthesis of novel pyrrole and pyrrolo[2,3-*d*]pyrimidine derivatives bearing sulfonamide moiety for evaluation as anticancer and radiosensitizing agents. Bioorg Med Chem Lett. 2010; 20:6316–6320. [PubMed: 20850308]

28. Gangjee A, Zhao Y, Lin L, Raghavan S, Roberts EG, Risinger AL, Hamel E, Mooberry SL. Synthesis and discovery of water-soluble microtubule targeting agents that bind to the colchicines site on tubulin and circumvent P-gp mediated resistance. J Med Chem. 2010; 53:8116–8128. [PubMed: 20973488]

29. Gangjee A, Kurup S, Ihnat MA, Thorpe JE, Shenoy SS. Synthesis and biological activity of N^4-phenylsubstituted-6-(2,4-dichlorophenylmethyl)-7*H*-pyrrolo[2,3-*d*]pyrimidine-2,4-diamines as vascular endothelial growth factor receptor-2 inhibitors and antiangiogenic and antitumor agents. Bioorg Med Chem. 2010; 18:3575–3587. [PubMed: 20403700]

30. Bennet SM, Nguyen-Ba N, Ogilvie KK. Synthesis and antiviral activity of some acyclic and C-acyclic pyrrolo[2,3-d]pyrimidine nucleoside analogues. J Med Chem. 1990; 33:2162–2173. [PubMed: 2165163]

31. Krawczyk SH, Nassiri MR, Kucera LS, Kern ER, Ptak RG, Wotring LL, Drach JC, Townsend LB. Synthesis and antiproliferative and antiviral activity of 2′-deoxy-2′-fluoroarabinofuranosyl analogs of the nucleoside antibiotics toyocamycin and sangivamycin. J Med Chem. 1995; 38:4106–4114. [PubMed: 7562946]

32. Hess S, Muller CE, Frobenius W, Reith U, Klotz K-N, Eger K. 7-deazaadenunes bearing polar substituents: structure-activity relationships of new A_1 and A_3 adenosine receptor antagonists. J Med Chem. 2000; 43:4636–4646. [PubMed: 11101355]

33. Bookser BC, Ugarkar BG, Matelich MC, Lemus RH, Allan M, Tsuchiya M, Nakane M, Nagahisa A, Wiesner JB, Erion MD. Adenosine kinase inhibitors. 6. Synthesis, water solubility, and antinociceptive activity of 5-phenyl-7-(5-deoxy-b-D-ribofuranosyl)pyrrolo[2,3-*d*]pyrimidines substituted at C4 with glycinamides and related compounds. J Med Chem. 2005; 48:7808–7820. [PubMed: 16302820]

34. Kim YA, Sharon A, Chu CK, Rais RH, Al Safarjalani ON, Naguib FNM, el Kouni MH. Structure-activity relationships of deaza-6-benzylthioinosine analogues as ligands of *Toxoplasma gondii* adenosine kinase. J Med Chem. 2008; 51:3934–3945. [PubMed: 18563892]

35. Gangjee A, Jain HD, Queener SF, Kisliuk RL. The effect of 5-alkyl modification on the biological activity of pyrrolo[2,3-*d*]pyrimidine containing classical and nonclassical antifolates as inhibitors of dihydrofolate reductase and as antitumor and/or antiopportunistic infection agents. J Med Chem. 2008; 51:4589–4600. [PubMed: 18605720]

36. Frolova LV, Evdokimov NM, Hayden K, Malik I, Rogelj S, Kornienko A, Magedov IV. One-pot multicomponent synthesis of diversely substituted 2-aminopyrroles. A short general synthesis of rigidins A, B, C, and D. Org Lett. 2011; 13:1118–1121. [PubMed: 21268660]

37. Mosmann T. Rapid colorimetric assay for cellular growth and survival - application to proliferation and cytotoxicity assays. J Immunol Methods. 1983; 65:55–63. [PubMed: 6606682]

38. See for example: Kemnitzer W, Drewe J, Jiang S, Zhang H, Wang Y, Zhao J, Jia S, Herich J, Labreque D, Storer R, Meerovitch K, Bouffard D, Rej R, Denis R, Blais C, Lamothe S, Attardo G, Gourdeau H, Tseng B, Kasibhatla S, Cai SX. Discovery of 4-aryl-4*H*-chromenes as a new series of apoptosis inducers using a cell- and caspase-based high-throughput screening assay. 1. Structure-activity relationships of the 4-aryl group. J Med Chem. 2004; 47:6299–6310. [PubMed: 15566300]

39. Jordan MA, Wilson L. Microtubules as a target for anticancer drugs. Nature Rev Cancer. 2004; 4:253–265. [PubMed: 15057285]

40. Hamel E. Evaluation of antimitotic agents by quantitative comparisons of their effects on the polymerization of purified tubulin. Cell Biochem Biophys. 2003; 38:1–22.

41. Lin CM, Ho HH, Pettit GR, Hamel E. The antimitotic natural products combretastatin A-4 and combretastatin A-2: studies on the mechanism of their inhibition of the binding of colchicine to tubulin. Biochemistry. 1989; 28:6984–6991. [PubMed: 2819042]

42. Tahir SK, Kovar SH, Ng RSC. Rapid colchicine competition-binding scintillation proximity assay using biotin-labeled tubulin. BioTechniques. 2000; 29:156–160. [PubMed: 10907090]

43. Löwe J, Li H, Downing KH, Nogales E. Refined structure of αβ-tubulin at 3.5 Å resolution. J Mol Biol. 2001; 313:1045–1057.

44. Bollag DM, McQueney PA, Zhu J, Hensens O, Koupal L, Liesch J, Goetz M, Lazarides E, Woods CM. Epothilones, a new class of microtubule-stabilizing agents with a taxol-like mechanism of action. Cancer Res. 1995; 55:2325–2333. [PubMed: 7757983]

45. Gigant B, Wang C, Ravelli RBG, Roussi F, Steinmetz MO, Curmi PA, Sobel A, Knossow M. Structural basis for the regulation of tubulin by vinblastine. Nature. 2005; 435:519–522. [PubMed: 15917812]

46. Horwitz SB, Cohen D, Rao S, Ringel I, Shen HJ, Yang CP. Taxol: mechanisms of action and resistance. J Natl Cancer Inst Monogr. 1993; 15:55–61. [PubMed: 7912530]

47. Kuppens IE. Current state of the art of new tubulin inhibitors in the clinic. Curr Clin Pharmacol. 2006; 1:57–70. [PubMed: 18666378]

48. Beckers T, Reissmann T, Schmidt M, Burger AM, Fiebig HH, Vanhoefer U, Pongratz H, Hufsky H, Hockemeyer J, Frieser M, Mahboobi S. 2-Aroylindoles, a novel class of potent, orally active small molecule tubulin inhibitors. Cancer Res. 2002; 62:3113–3119. [PubMed: 12036922]

49. Hande KR, Hagey A, Berlin J, Cai Y, Meek K, Kobayashi H, Lockhart AC, Medina D, Sosman J, Gordon GB, Rothenberg ML. The pharmacokinetics and safety of ABT-751, a novel, orally bioavailable sulfonamide antimitotic agent: results of a phase 1 study. Clin Cancer Res. 2006; 12:2834–2840. [PubMed: 16675578]

50. Rupp C, Steckel H, Mueller BW. Solubilization of poorly water-soluble drugs by mixed micelles based on hydrogenated phosphatidylcholine. Int J Pharm. 2010; 395:272–280. [PubMed: 20580793]

51. Mueller CE. Prodrug approaches for enhancing the bioavailability of drugs with low solubility. Chem Biodiversity. 2009; 6:2071–2083.

52. For a recent example see: Regina G, Bai R, Rensen WM, Di Cesare E, Coluccia A, Piscitelli F, Famiglini V, Reggio A, Nalli M, Pelliccia S, Da Pozzo E, Costa B, Granata I, Porta A, Maresca B, Soriani A, Iannitto ML, Santoni A, Li J, Cona MM, Chen F, Ni Y, Brancale A, Dondio G, Vultaggio S, Varasi M, Mercurio C, Martini C, Hamel E, Lavia P, Novellino E, Silvestri R. Toward Highly Potent Cancer Agents by Modulating the C-2 Group of the Arylthioindole Class of Tubulin Polymerization Inhibitors. J Med Chem. 2013; 56:123–149. [PubMed: 23214452]

53. See for example: Romagnoli R, Baraldi PG, Salvador MK, Preti D, Tabrizi MA, Brancale A, Fu X-H, Li J, Zhang S-Z, Hamel E, Bortolozzi R, Basso G, Viola G. Synthesis and evaluation of 1, 5-disubstituted tetrazoles as rigid analogues of combretastatin A-4 with potent antiproliferative and antitumor Activity. J Med Chem. 2012; 55:475–488. [PubMed: 22136312]

54. Harker WG, Sikic BI. Multidrug (pleiotropic) resistance in doxorubicin-selected variants of the human sarcoma cell line MES-SA. Cancer Research. 1985; 45:4091–4096. [PubMed: 4028002]

55. Verdier-Pinard P, Lai J-Y, Yoo H-D, Yu J, Marquez B, Nagle DG, Nambu M, White JD, Falck JR, Gerwick WH, Day BW, Hamel E. Structure-activity analysis of the interaction of curacin A, the potent colchicine site antimitotic agent, with tubulin and effects of analogs on the growth of MCF-7 breast cancer cells. Mol Pharmacol. 1998; 53:62–67. [PubMed: 9443933]
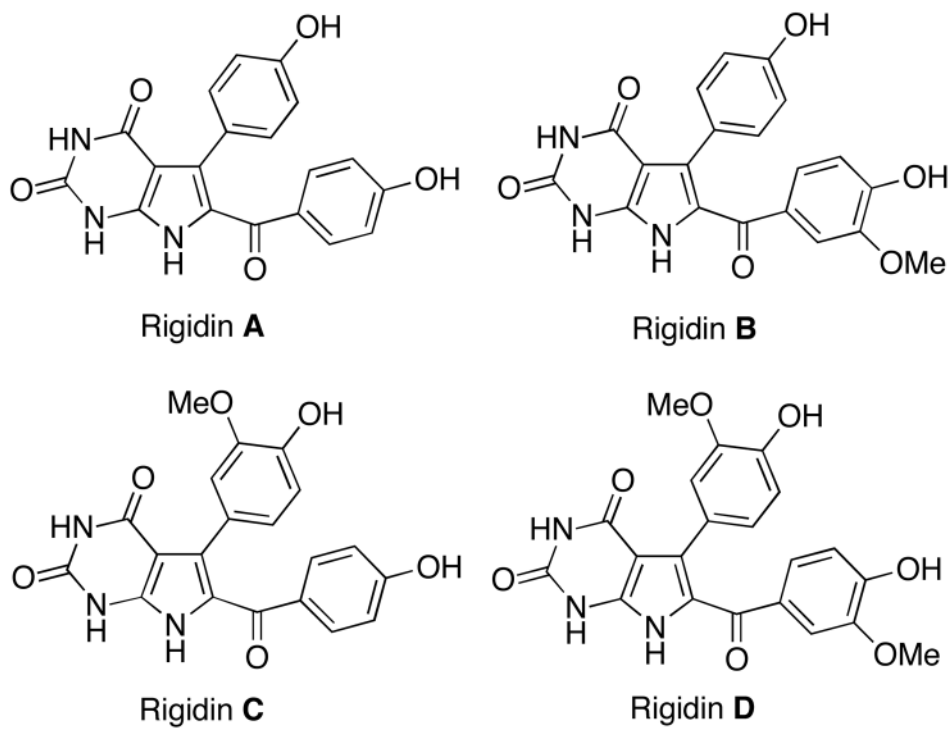
Figure 1.
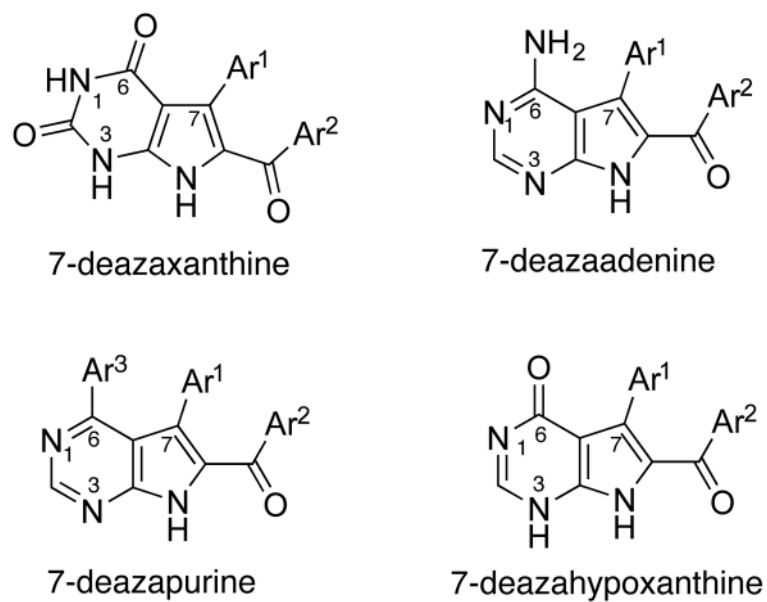Structures of rigidins A, B, C and D

Figure 2.
Structures of pyrrolo[2,3-*d*]pyrimidines prepared in this work
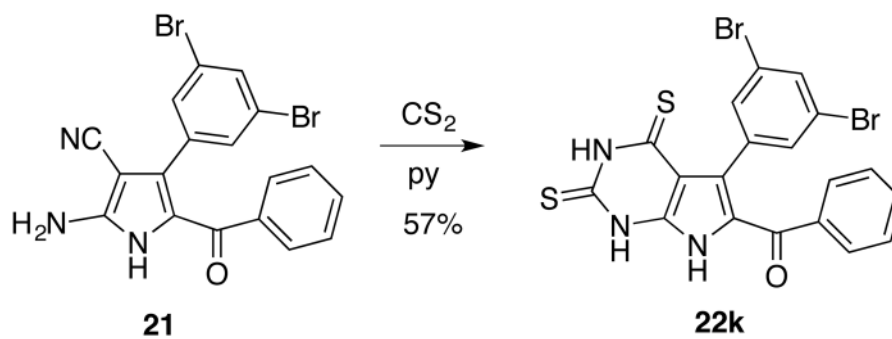
Figure 3.
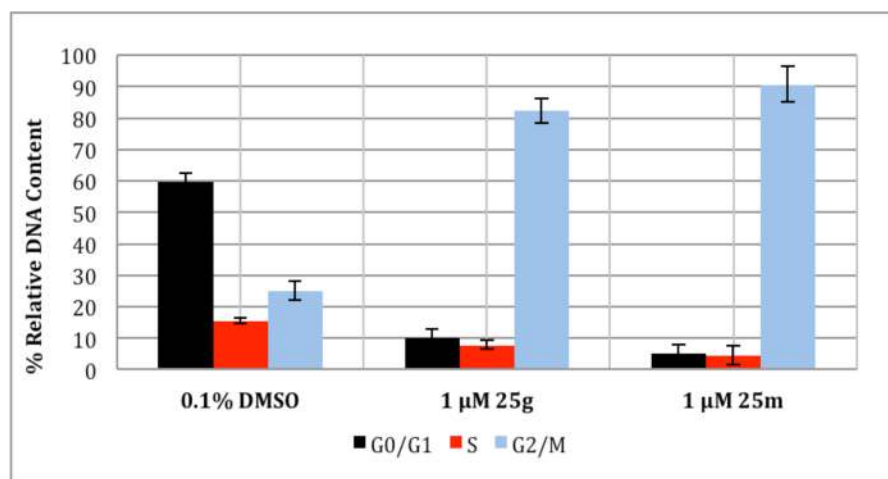Preparation of an additional 7-deazapurine **22k**

Figure 4.
Flow cytometric cell cycle analysis using HeLa cells treated for 32 h with **25g** or **25m**. Error bars represent the standard error between triplicate experiments.
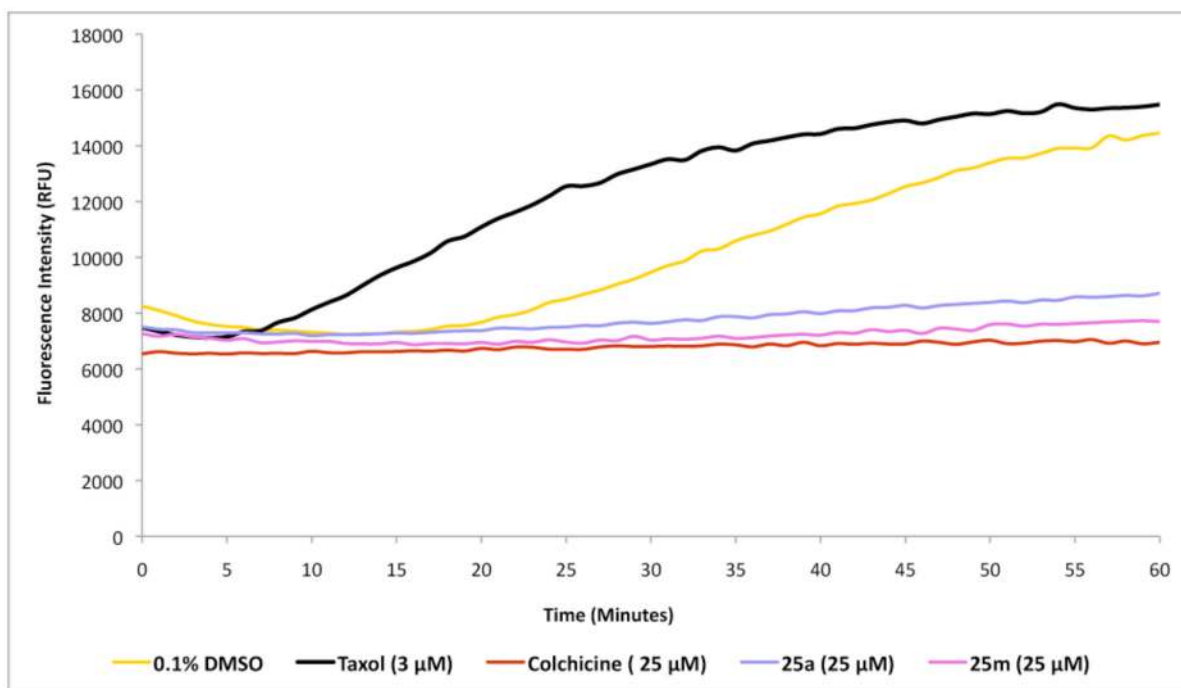
Figure 5.
Effect of **25a** and **25m** on *in vitro* tubulin polymerization. Taxol (3 μM) promotes microtubule formation relative to 0.1% DMSO control. **25a** (25 μM)**, 25m** (25 μM) and colchicine (25 μM) completely suppress tubulin polymerization.
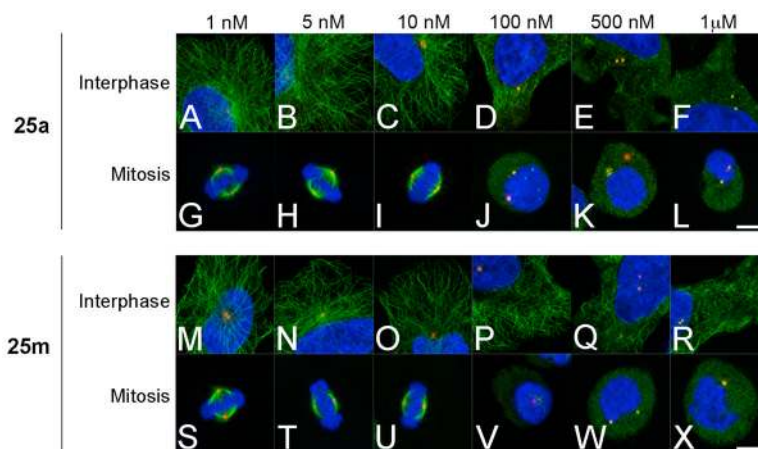
Figure 6.
Microtubule organization in HeLa cells during interphase and mitosis. HeLa cells were treated for 3 h with compound **25a** (panels A–L) and **25m** (M–X) at a range of concentrations. Following drug treatment, cells were probed for microtubules (green), the centrosome marker pericentrin (red) and DNA (blue). Bar, 10 μm.

Table 1

MCR-based total general synthesis of rigidins A–D and their first-generation 7-deazaxanthine synthetic analogues **22a–j**
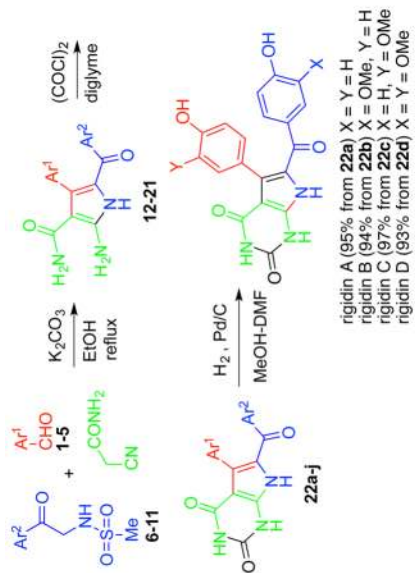
aldehyde	methanesulfonylamide	pyrrole	7-deazaxanthine	Ar¹	Ar²	overall yield %
1	6	12	22a	OBn	OBn	64
1	7	13	22b	OBn	OMe, OBn	62
2	6	14	22c	OMe, OBn	OBn	62
2	7	15	22d	OMe, OBn	OMe, OBn	57
3	8	16	22e	OMe, OMe, OMe	F	74

aldehyde	methanesulfonylamide	pyrrole	7-deazaxanthine	Ar¹	Ar²	overall yield %
3	9	17	22f	OMe, OMe, OMe	Br	64
3	7	18	22g	OMe, OMe, OMe	OMe, OBn	59
4	10	19	22h	OMe	OMe	57
4	11	20	22i	OMe	Ph	62
5	11	21	22j	Br, Br	Ph	43

rigidin A (95% from **22a**) X = Y = H
rigidin B (94% from **22b**) X = OMe, Y = H
rigidin C (97% from **22c**) X = H, Y = OMe
rigidin D (93% from **22d**) X = Y = OMe

Table 2

4-CR leading to the formation of the second-generation analogues based on the 7-deazaadenine skeleton.
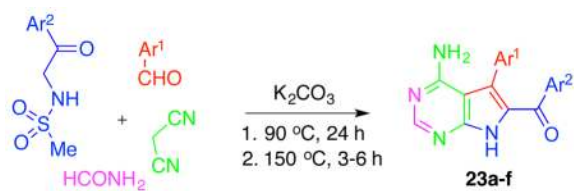
7-deazaadenine	Ar[1]	Ar[2]	% yield
23a		Ph	58
23b		Ph	66
23c	Ph	Ph	48
23d		Ph	85
23e			54
23f		Ph	72

Table 3

4-CR leading to the formation of the second-generation analogues based on the 7-deazapurine skeleton.

6,7-dideazaadenine	Ar¹	Ar²	Ar³	% yield
24a	—⟨⟩—OMe	—⟨⟩—OMe	—⟨⟩—OMe	63
24b	—⟨⟩—OMe	Ph	Ph	30
24c	3,5-diBr-phenyl	Ph	—⟨⟩—Me	33
24d	3,5-diBr-phenyl	Ph	Ph	39
24e	pyridin-3-yl	Ph	Ph	22

Table 4

4-CR leading to the formation of the second-generation analogues based on the 7-deazahypoxanthine skeleton.
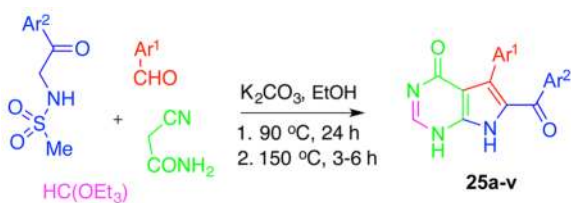
7-deazahypoxanthine	Ar¹	Ar²	% yield
25a	Ph	Ph	71
25b		Ph	68
25c		Ph	61
25d		Ph	54
25e		Ph	53
25f		Ph	60
25g		Ph	88
25h		Ph	61
25i		Ph	64
25j		Ph	37

7-deazahypoxanthine	Ar¹	Ar²	% yield
25k	Br, OMe, OMe	Ph	51
25l	Cl, Cl	Ph	74
25m	Br, Br	Ph	77
25n	OH	Ph	26
25o	CN	Ph	47
25p	Br, Br	F	56
25q	OMe, OMe, OMe	OMe	56
25r	Br, Br	OMe	60
25s	Br, Br	OBn	61

7-deazahypoxanthine	Ar¹	Ar²	% yield
25t	3,5-dibromophenyl	4-bromophenyl	54
25u	Ph	4-OBn phenyl	68
25v	4-bromothiophen-2-yl	Ph	71

Table 5

4-CR with concomitant debenzylation leading to the formation of hydroxyl-substituted 7-deazahypoxanthine analogues.
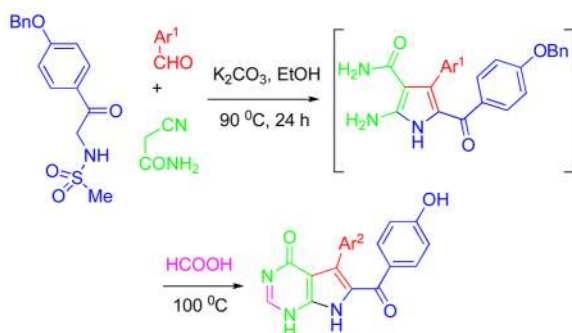
7-deazahypoxanthine	Ar¹	Ar²	% yield
25w	Ph	Ph	88
25x	(3,5-dibromophenyl)	(3,5-dibromophenyl)	70
25y	(3-OMe, 4-OBn phenyl)	(3-OMe, 4-OH phenyl)	64
25z	(4-OBn phenyl)	(4-OH phenyl)	71

Table 6

Antiproliferative activities of the synthesized 7-deazapurines

7-deazapurine	cell viability[a] GI_{50}, µM	
	HeLa	**MCF-7**
rigidin A	> 100	> 100
rigidin B	> 100	> 100
rigidin C	> 100	> 100
rigidin D	> 100	> 100
22e	> 100	> 100
22f	> 100	> 100
22g	> 100	> 100
22h	> 100	> 100
22i	80 ± 10	14 ± 1
22j	71 ± 12	47 ± 5
22k	> 100	> 100
23a	> 100	> 100
23b	> 100	> 100
23c	4.4 ± 0.4	3.9 ± 0.5
23d	28 ± 4	15 ± 0
23e	> 100	> 100
23f	> 100	> 100
24a	20 ± 1	8.0 ± 1
24b	70 ± 15	75 ± 11
24c	9.0 ± 1	7.0 ± 1
24d	18 ± 10	10 ± 2
24e	45 ± 9	51 ± 2
25a	0.035 ± 0.007	0.040 ± 0.024
25b	0.2 ± 0.1	0.150 ± 0.060
25c	0.10 ± 0.07	0.06 ± 0.02
25d	0.13 ± 0.05	0.06 ± 0.02
25e	0.065 ± 0.010	0.070 ± 0.025
25f	0.15 ± 0.05	0.135 ± 0.075
25g	0.080 ± 0.025	0.087 ± 0.020
25h	0.88 ± 0.06	1.26 ± 0.18
25i	48 ± 8	33 ± 4
25j	8.2 ± 1	40 ± 4
25k	7.1 ± 1	10 ± 5
25l	4.9 ± 0.3	2.2 ± 0.1
25m	0.095 ± 0.040	0.095 ± 0.010
25n	0.86 ± 0.06	1.09 ± 0.12
25o	0.19 ± 0.01	0.25 ± 0.02
25p	6.3 ± 1	0.80 ± 0.01

7-deazapurine	cell viability[a] GI$_{50}$, μM	
	HeLa	**MCF-7**
25q	>100	7.0 ± 1
25r	0.30 ± 0.07	0.11 ± 0.035
25s	0.40 ± 0.01	0.31 ± 0.01
25t	2.2 ± 1	0.6 ± 0.1
25u	0.045 ± 0.004	0.053 ± 0.005
25v	43 ± 6	56 ± 2
25w	0.4 ± 0.1	0.3 ± 0.07
25x	0.30 ± 0.01	0.26 ± 0.05
25y	5.0 ± 0.6	3.0 ± 0.6
25z	4.0 ± 0.6	2.8 ± 0.8

[a]Concentration required to reduce the viability of cells by 50% after a 48 h treatment with the indicated compounds relative to a DMSO control ± SD from two independent experiments, each performed in 4 replicates, as determined by the MTT assay.

Table 7

Inhibition of tubulin assembly and colchicine binding to β-tubulin

compound	inhibition of tubulin assembly[b]	inhibition of colchicine binding[c]	
	IC$_{50}$ (μM) ± SD	% inhibition ± SD	
		5 μM inhibitor	1 μM inhibitor
CA-4[a]	0.96 ± 0.07	99 ± 0.4	89 ± 0.6
25a	1.2 ± 0.1	88 ± 0.7	58 ± 4
25m	1.6 ± 0.04	71 ± 0.5	ND

[a]CA-4 = combretastatin A-4.

[b]Inhibition of tubulin polymerization by selected compounds. Tubulin was at 10 μM.

[c]% Inhibition of [^{3}H]colchicine (5 μM) binding to tubulin (1 μM) by selected compounds.

Table 8

Antiproliferative effect of selected compounds against MDR cells

	GI$_{50}$ *in vitro* Values (nM)[a]	
	MES-SA	MES-SA/Dx5
Taxol	7 ± 1	9800 ± 283
Vinblastine	6 ± 1	5000 ± 1414
25m	81 ± 6	394 ± 10
25a	30 ± 4	70 ± 4

[a]Concentration required to reduce the viability of cells by 50% after a 48 h treatment with the indicated compounds relative to a DMSO control ± SD from two independent experiments, each performed in 4 replicates, as determined by the MTT assay.

Table 9

Antiproliferative properties of potent 7-deazahypoxanthines **25** against cancer cell lines representing cancers with dismal prognoses or derived from tumor metastases

| compound | glioma | | melanoma | | NSCLC | head and neck cancer | | | head and neck metastases | |
	U373	Hs683	SKMEL-28	B16F10	A549	UM-SCC10A	UM-SCC22A	UM-SCC10B	UM-SCC22B	
25m	30	20	20	50	30	90	110	100	20	
25g	30	20	20	40	20	90	120	130	20	
25a	<10	10	<10	20	10	ND	ND	ND	ND	

GI$_{50}$ in vitro values (nM)[a]

[a] Concentration required to reduce the viability of cells by 50% after a 48 h treatment with the indicated compounds relative to a DMSO control, as determined by the MTT assay